THE GEOLOGICAL SOCIETY OF AMERICA®

Observations and Analyses of the 9 January 2018 Debris-Flow Disaster, Santa Barbara County, California

JEREMY T. LANCASTER*

California Geological Survey, 801 K Street, Sacramento, CA 95820

BRIAN J. SWANSON

California Geological Survey, 320 West 4th Street, Suite 850, Los Angeles, CA 90013

STEFANI G. LUKASHOV

California Geological Survey, 801 K Street, Sacramento, CA 95820

NINA S. OAKLEY

Center for Western Weather and Water Extremes, Scripps Institution of Oceanography, 9500 Gilman Drive, La Jolla, CA 92093

JACOB B. LEE

California Geological Survey, 6105 Airport Road, Redding, CA 96002

ELEANOR R. SPANGLER

California Geological Survey, 801 K Street, Sacramento, CA 95820

JANIS L. HERNANDEZ
BRIAN P. E. OLSON
MIKE J. DEFRISCO

California Geological Survey, 320 West 4th Street, Suite 850, Los Angeles, CA 90013

DONALD N. LINDSAY

California Geological Survey, 6105 Airport Road, Redding, CA 96002

YONNI J. SCHWARTZ

U.S. Forest Service, 1190 East Ojai Avenue, Ojai, CA 93023

SOLOMON E. MCCREA
PETER D. ROFFERS
CHRISTOPHER M. TRAN

California Geological Survey, 801 K Street, Sacramento, CA 95820

Key Terms: ***Post-Fire, Debris Flows, Alluvial Fan, Narrow Cold Frontal Rain Band, Rainfall Intensity, Inundation, Montecito, Thomas Fire, Loss Estimate***

1

*Corresponding author email: xxxx@xxxx

ABSTRACT

The post–Thomas Fire debris flows of 9 January 2018 killed 23 people, damaged 558 structures, and caused severe damage to infrastructure in Montecito and Carpinteria, CA. U.S. Highway 101 was closed for 13 days, significantly impacting transportation and commerce in the region. A narrow cold frontal rain band generated extreme rainfall rates within the western burn area, triggering runoff-driven debris flows that inundated 5.6 km^2

of coastal land in eastern Santa Barbara County. Collectively, this series of debris flows is comparable in magnitude to the largest documented post-fire debris flows in the state and cost over a billion dollars in debris removal and damages to homes and infrastructure. This study summarizes observations and analyses on the extent and magnitude of inundation areas, debris-flow velocity and volume, and sources of debris-flow material on the south flank of the Santa Ynez Mountains. Additionally, we describe the atmospheric conditions that generated intense rainfall and use precipitation data to compare debris-flow source areas with spatially associated peak 15 minute rainfall amounts. We then couple the physical characterization of the event with a compilation of debris-flow damages to summarize economic impacts.

INTRODUCTION

Late autumn and winter wildfires in California create a challenging situation for emergency managers because storms may impact a burn area while emergency response to wildfire is still in progress. The Thomas Fire created this challenge in Ventura and Santa Barbara counties, burning 281,893 acres, with full containment declared on 12 January 2018. A Presidential Disaster Declaration was issued on 8 December 2017. On 6 January 2018, the National Weather Service issued a flash-flood watch for the burn area with anticipated 1 hour rainfall rates of 0.5 to 1.0 in./hr (12.7 to 25.4 mm/hr) (Laber, 2018), just below the U.S. Geological Survey's (USGS) minimum Santa Barbara region debris-flow triggering rate of 1.2 in./hr (30.5 mm/hr) at the 15 minute duration
2 (Staley, 2018). As the storm moved onshore during the morning of 9 January, intense rainfall associated with a narrow cold frontal rain band (NCFR) passed through eastern Santa Barbara County and western Ventura County, triggering debris flows and sediment-laden flows on steep burned slopes within the Thomas Fire perimeter (Figure 1). The most destructive flows originated on the south flank of the Santa Ynez Mountains and rapidly coalesced into the major canyons that drain southward into the communities of Montecito, Summerland, and Carpinteria, CA. The flows overwhelmed debris-retention basins, clogged culverts and bridge crossings, and overtopped existing channel banks, causing widespread inundation onto fan areas of the Montecito and Carpinteria piedmonts (Figure 2). The flows killed 23 people, damaged or destroyed 558 structures, inundated and closed U.S. Highway 101 (U.S. 101) for 13 days, damaged infrastructure, and disrupted all utility services in the area, including damage to a high-pressure gas line at San Ysidro Creek that resulted in a large explosion and fire. Emergency response personnel conducted 800 rescues on the morning of the event (SBC, 2018a, 2018b).

Following the debris-flow event, the County of Santa Barbara requested assistance from the State of California, Governor's Office of Emergency Services, to assess impacted areas in the communities of Montecito and Carpinteria, including support for evacuation planning efforts.

This study summarizes observations and analyses conducted by the California Geological Survey (CGS) and affiliates to document the large-magnitude debris-flow event in the coastal plain of eastern Santa Barbara County. We incorporate the results of previous assessments published in CAL FIRE (2018a), Kean et al. (2019), and Lukashov et al. (2019), and new data to provide a summary report of debris-flow inundation, runout, velocity, volume, and source area observations; analyses of debris-flow source distribution and triggering rainfall; and documentation of direct and indirect damages and preliminary cost estimates associated with direct damages.

Background

In California, the most dangerous consequences of alluvial-fan flooding are often underestimated in the land-use planning process in favor of developing prime real estate. Riverine flood hazard paradigms have been applied to western steeplands that issue onto alluvial fans built by successive debris-laden flood and debris-flow deposits, forming the sole regulatory framework used in the planning and mitigation process while creating residual risk (AFTF, 2010). Wildfires create the opportunity for one of those consequences—post-fire debris flows (PFDFs), which are a common threat to southern California communities due to urbanization of alluvial-fan floodplains (USGS, 2005; Lancaster et al., 2015). Examples of PFDF impacts in California including the 1934 New Year's Day event in the La Crescenta Valley, Los Angeles County (Chawner, 1934), the 1981 Mill Creek disaster in the San Gabriel Mountains (Shuirman and Slosson, 1992), the 25 December 2003 Christmas Day event in San Bernardino, San Bernardino County (Oakley et al., 2017), and the 12 July 2008 Oak Creek event in Inyo County (Wagner et al., 2012).

While storm totals are primary drivers for flooding and hillslope processes in unburned settings, PFDFs are often triggered by rainfall durations of 30 minutes or less (Moody and Martin, 2001; Kean et al., 2011), with little lag time between peak 15 minute rainfall and the passage of the debris flows (Kean et al., 2011). This short-duration and high-intensity rainfall causes impacts to denuded hillslopes and soils, including the

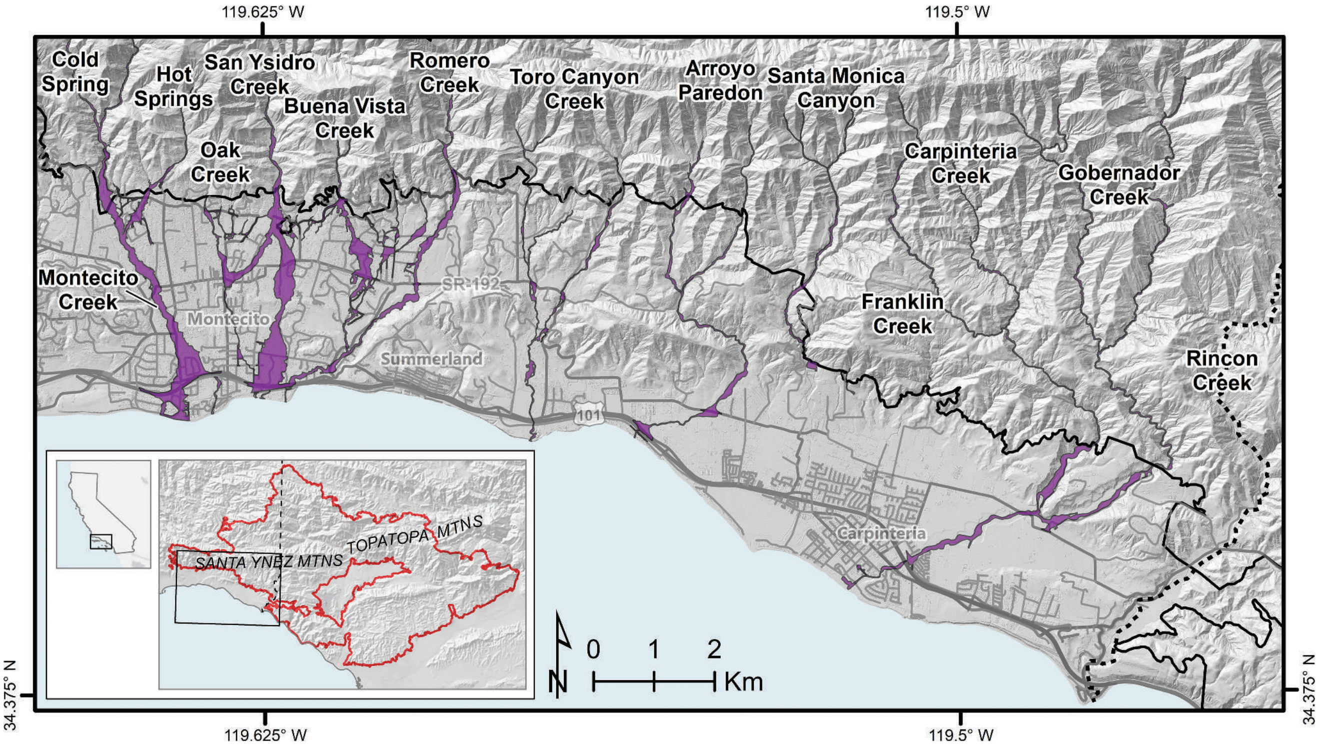

Figure 1. Overview map of the study area between Montecito Creek in the west and Rincon Creek in the east, showing inundation from the 9 January 2018 debris flows in purple, the Thomas Fire perimeter in black, and the names of the canyons draining to the coastal communities of Montecito, Summerland, and Carpinteria, CA. The county line is defined by the black dashed line along Rincon Creek on the east side of the map. Thomas Fire burn area is shown on inset map.

dislocation of soil particles, initiation of fine-scale slope failures, concentration of runoff, and the development of rills that transition into gullies downslope. Ultimately, this process leads to the formation of surge fronts that build into massive walls of mud and water (Kean et al., 2011, 2013; Staley et al., 2013). With the addition of cobbles and boulders, these flows take on two phases—a fluidized matrix of ash, water, and fine-grained sediment, and a solid phase of cobbles and boulders; flows grow in size by entraining additional soil, rock, and vegetative matter from channel beds and banks. Where surge fronts interact with drainage infrastructure and roads, they can avulse into areas of human occupancy, tearing homes off their foundations and carrying cars and unanchored anthropogenic features downstream.

Figure 2. Damaged home along Buena Vista Creek sitting among a debris-flow boulder field and abundant woody debris. Mud line on building is asymmetric, indicating surge-front depths were greater on the left side of the structure (near the top of the handrail on upper floor deck) than on the right side (photo: Brian Swanson, CGS; all photos taken by USGS and CGS unless otherwise noted).

PHYSICAL SETTING

Topography, Climate, and Geology

The study area is in the western part of the Thomas Fire burn area, consisting of large canyons on the south flank of the east-west–trending Santa Ynez Mountains, which drain across the adjacent Santa Barbara Coastal Plain into the Santa Barbara Channel. These canyons include, from west to east, Cold Spring, Hot Springs, Oak, San Ysidro, Buena Vista, Romero, Toro, Arroyo Paredon, Santa Monica, Franklin, Carpinteria, Gobernador, and Rincon creeks. Rincon Creek generally defines the Santa Barbara–Ventura County boundary (Figure 1). Elevations at the crest of the Santa Ynez Mountains range

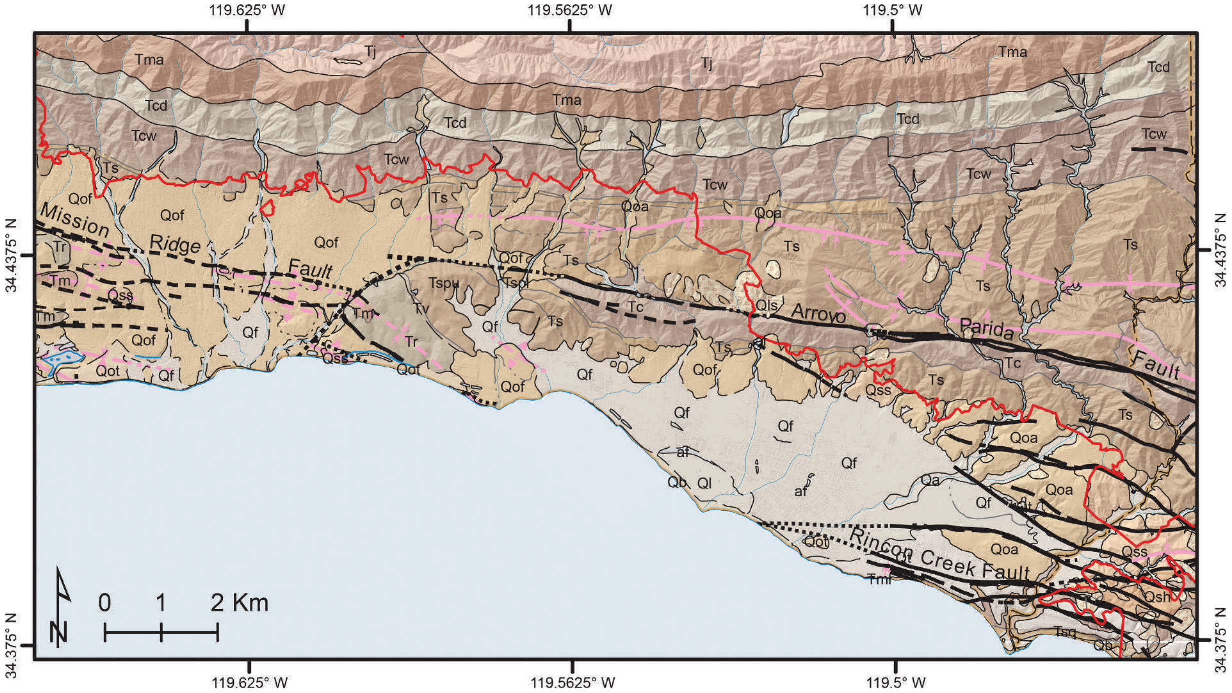

Figure 3. Regional geologic map of Santa Barbara coastal area. Geologic map units underlying the source areas include Eocene-age Juncal Formation (Tj), Matilija Formation (Tma), Cozy Dell Formation (Tcd), Coldwater Formation (Tcw); late Miocene–age Sespe Formation (Ts), Vaqueros Formation (Tv), Modelo Formation (Tm); Pliocene to Pleistocene–age undifferentiated sandstone (Qss); Quaternary surficial deposits, including Pleistocene- to Holocene-age deposits, including alluvial fan (Qof) and valley alluvium (Qoa); and Holocene-age deposits, including alluvial-fan (Qf) and alluvial-valley deposits (Qa). Dark-red line depicts the fire perimeter boundary from the Thomas Fire. Faint-black lines are geologic unit contacts, and dark-black lines depict faults, solid where accurately located, dashed where inferred, dotted where concealed.

from about 1,067 m (3,500 ft) above Montecito up to 1,463 m (4,800 ft) near the headwaters of Rincon Creek.

The area has a typical Mediterranean climate with warm dry summers and cool wet winters, where precipitation occurs almost entirely as rain. Mean annual precipitation ranges from 29.7 in. (75.4 cm) at Juncal Dam in the Santa Ynez Mountains (2,240 ft above sea level [682.7 m]) to 17.7 in. (45 cm) in Santa Barbara (5 ft above sea level [1.5 m]) (WRCC, 2017). This difference in mean annual precipitation demonstrates the strong topographic influence on precipitation in the area. Mean annual precipitation for Montecito is 19.8 in. (50.3 cm) (SBCFCD, 2020).

The Santa Ynez Mountains are underlain by a sequence of steeply tilted, east-west–trending Cretaceous to Miocene sedimentary strata (Figure 3; Minor et al., 2009). Formations include Cretaceous unnamed sandstone, mudstone, and conglomerate, which are overlain to the south in succession by the Eocene marine fine-grained Juncal Formation, sandstone-dominated Matilija Formation, fine-grained Cozy Dell Shale, and sandstone-dominated Coldwater Formation, and Oligocene to early Miocene nonmarine sandstone and mudstone of the Sespe Formation (Dibblee, 1966, 1982).

Geomorphology

Alluvial fans are categorized as streamflow fans, debris fans, and composite fans based on their geomorphology and origin (Bull, 1977; NRC, 1996). Debris-flow–dominated fans have steeper gradients (generally $\geq 6°$, or 10.5 percent) built by successive debris flows and sediment-gravity deposits, with water-borne sediment concentrations generally greater than 50 percent by volume (Pierson and Costa, 1987; Iverson, 1997). Catchment morphometric parameters such as Melton's number when combined with planimetric length can be used to classify fans that are susceptible to debris flows and debris floods (Wilford et al., 2004; Welsh and Davies, 2011). Alluvial fans dominated by fluvial processes, debris floods and debris flows may be categorized by Melton's numbers of <0.3, 0.3–0.6 and >0.6, respectively, with planimetric lengths of <2.7 km for debris-flow–dominated watersheds and >2.7 km for fluvial- and debris-flood–dominated watersheds (Welsh and Davies, 2011).

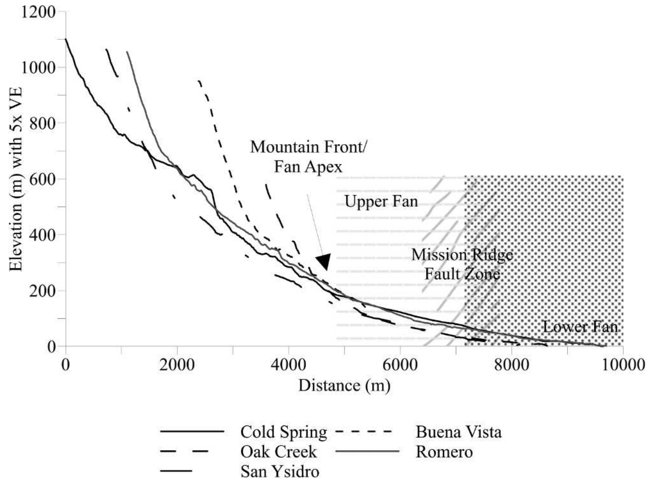

Figure 4. Longitudinal profiles from west to east (left to right) through Montecito piedmont aligned to the mountain front/fan apices, showing the steeper composite fans separated by the more gently sloping streamflow fans due to the crustal warping on the Mission Ridge Fault Zone; Cold Spring and Montecito creeks are combined, and Hot Springs Creek is not shown.

Table 1. *Watershed data including planimetric length, relief ratio, Melton's number, and drainage area, showing a general lengthening of watersheds from canyon mouth to crest, and a general decrease in relief ratio and Melton's number moving eastward from Montecito through Carpinteria, CA.*

Watershed	Planimetric Length (km)	Relief Ratio	Melton's Number	Drainage Area (km^2)
Montecito area				
Cold Spring	3.55	0.20	0.27	9.35
Hot Springs	2.16	0.30	0.57	1.62
Oak Creek	1.13	0.34	0.57	0.48
San Ysidro	3.67	0.22	0.32	7.80
"Buena Vista"	2.26	0.30	0.56	1.76
Romero	3.03	0.23	0.38	4.89
Summerland and Carpinteria				
East Toro	4.39	0.19	0.32	8.43
Arroyo Paredon	5.20	0.15	0.34	9.05
Santa Monica	5.21	0.17	0.34	8.97
Franklin Creek	1.75	0.19	0.32	2.03
Carpinteria Creek	6.36	0.13	0.31	12.79
Gobernador Creek	6.79	0.11	0.26	18.73
Rincon Creek	9.01	0.11	0.27	22.73

The geomorphic character of the study area is dominated by large south-draining watershed catchments on the south flank of the Santa Ynez Mountains and the broad piedmont of the Santa Barbara Coastal Plain, which extends from the mountain front to the coastline (see Figures 4 and 5 for Montecito and Carpinteria/Summerland areas, respectively). Planimetric lengths of the watersheds range from about 1 to almost 3.7 km above Montecito; near Toro Canyon, the mountain front shifts to the south, and the primary catchments increase in length, ranging up to 9 km above Carpinteria at Rincon Creek (see Table 1). Toro Canyon is an antecedent drainage that cuts through

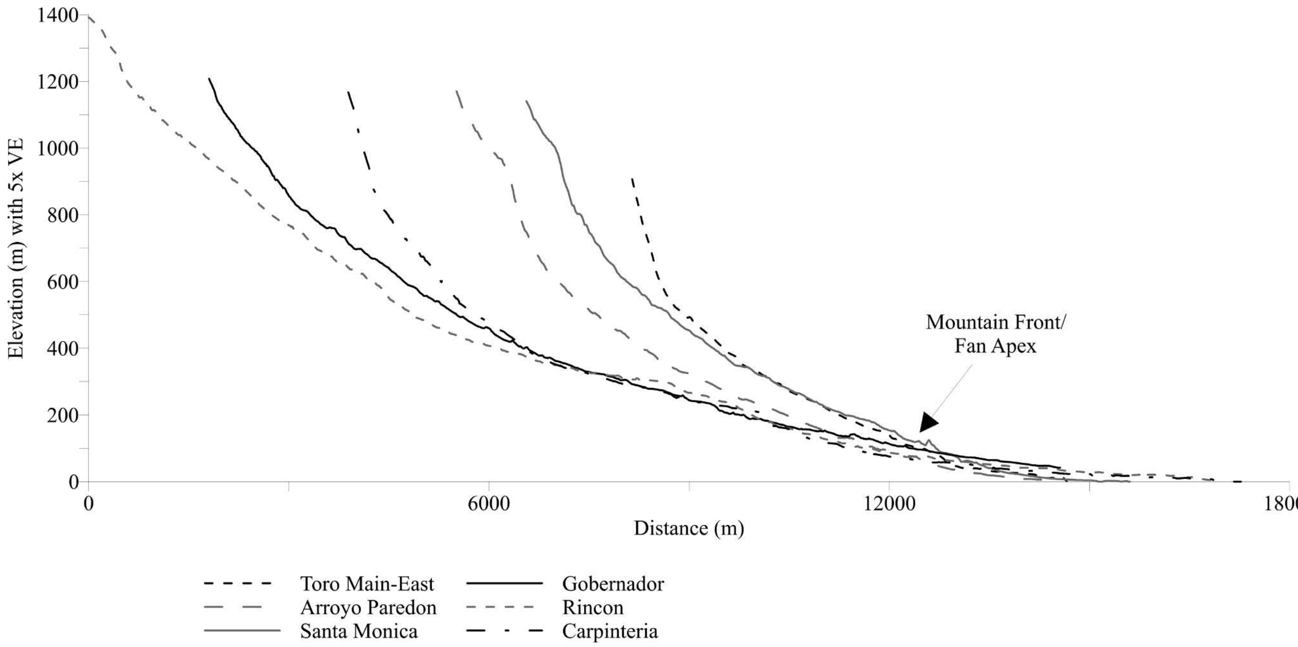

Figure 5. Longitudinal profiles through the Summerland and Carpinteria piedmonts showing a doubling in watershed length from west to east upstream of the apices. The length of the entire Toro flow path is 6.5 km, and the length of the entire Carpinteria flow path is 13.4 km. Gobernador Creek, a tributary to Carpinteria Creek, is not shown.

a ridge uplifted along the Arroyo Parida Fault. Arroyo Paredon is deflected eastward by the same uplifted ridge, and canyons farther east show varying degrees of less prominent reorientation along the fault trace. Longitudinal channel profiles for each drainage are illustrated in Figures 4 and 5.

South of the mountain front, much of the piedmont is underlain by alluvial-fan deposits that formed where steep, topographically confined drainages transition to flatter, unconfined terrain. Debris from sediment-laden flows and debris flows accumulates along distributary channels to construct the landform over time, and fans from adjacent canyons coalesce to form a bajada. Fan surfaces range from active to relict, and channels are typically entrenched into older deposits at the fan apices.

At Montecito, the piedmont plain is bisected by a discontinuous alignment of low hills uplifted along the Mission Ridge Fault (MRF) during Quaternary time (see pink shaded area on Figure 6). Alluvial fans grade from their apices at the mountain front to the MRF, where distributary fan drainage patterns transition to several confined antecedent channels through this zone of uplift. North of the uplift, upper fan channel gradients generally increase with decreasing drainage size, ranging from 5.3 percent to 6.7 percent (2.9° to 3.8°) below the large canyons of Cold Spring and San Ysidro canyons, respectively, to 7.6 percent (4.3°), 9.1 percent (5.2°), and 12 percent (6.8°) below the smaller canyons of Romero, Oak Creek, and Buena Vista Creek, respectively (Figure 6). Alluvial fans in the Montecito plain range in size from approximately 0.20 km^2 to 1.75 km^2.

South of the MRF, the drainage system is less constrained, forming a series of secondary fan apices and streamflow fans of relatively lower gradient. Lower fan channel gradients range from 2.7 percent to 3.1 percent (1.5° to 1.8°) south of Mission Ridge. These streamflow fans range in size from 0.2 km^2 to 0.9 km^2, with the largest emerging from Montecito Creek (active surfaces make up less than 0.5 km^2 of the fan), although San Ysidro Creek has a larger active surface at 0.7 km^2.

East of Montecito, upper fan gradients are generally lower and increase with decreasing drainage size, ranging from 1.8 percent to 2.6 percent (1.0° to 1.5°) below the larger canyons of Carpinteria and Gobernador, respectively, and 3.4 percent to 10.3 percent (2.0° to 5.9°) below the smaller drainages. Where the drainage systems are less constrained, and late Pleistocene to Holocene units consist primarily of distal lower fan deposits and alluvial valley deposits, gradients range from 0.8 percent to 5.4 percent (0.5° to 3.1°) (Figures 5 and 7). The Arroyo Paredon fan is similar in size to the larger fans in Montecito, at approximately 1.7 km^2, while to the east, the alluvial fan of Santa Monica Creek is the largest in the study area at 2.8 km^2. To the east and west of these fans, both Franklin and Toro Canyon alluvial fans are much smaller at about 0.3 km^2.

Morphometric Relationships

Morphometric parameters, including Melton's number, planimetric length, and fan gradient, were extracted for the Santa Barbara Coastal Plain watersheds to assess flow processes controlling alluvial-fan formation (see Table 1 and Figure 8). In general, Melton's number ranges from 0.26 to 0.57, and planimetric length ranges from 1.3 to 9.0 km, with the median of the data at 0.37 and 4.1 km, respectively, which suggests that most of these watersheds are dominated by fluvial/debris-flood processes per criteria in Welsh and Davies (2011). Planimetric lengths of these watersheds increase and the Melton's number decreases systematically from west to east, suggesting that they become progressively more streamflow dominated to the east. In contrast, Hot Springs, Oak, and Buena Vista Canyon watersheds above Montecito exhibit Melton's numbers and planimetric length of 0.3 to 0.6 and less than 2.7 km, respectively, which indicate their fan landforms are debris flow dominated. Upper alluvial fan gradients at Montecito and at Toro and Santa Monica canyons to the east are generally ≥4° (7 percent), indicating that past debris-flow processes are a component of fan formation, which was confirmed by field observations.

Wildfire-induced perturbations are known to systematically influence morphometric thresholds correlated with debris-flow generation. For example, a regression study by Gartner et al. (2014) suggested that PFDF occurrence and magnitude are correlated with Melton's number ranging from 0.05 to 0.71 (with an average of 0.25), and the planimetric length ranges from 0.2 to 12.9 km (with an average of 3.4 km). The watershed morphometric data from the Santa Barbara watersheds generally fall within these ranges, but they indicate the influence of wildfire on geomorphic thresholds as they fall well below the debris-flow thresholds described in Welsh and Davies (2011).

Fire and Debris-Flow History

Debris flows and/or flooding have inundated portions of Santa Barbara County more than twenty times since 1900 (USACE, 1999; Gurrola and Rogers, 2020), with wildfire exacerbating the effects of flooding and damaging debris flows on the coastal plain in the winters of 1914, 1926, 1964, 1969, 1971, 2017, and 2018. Events are not always widespread, with localized

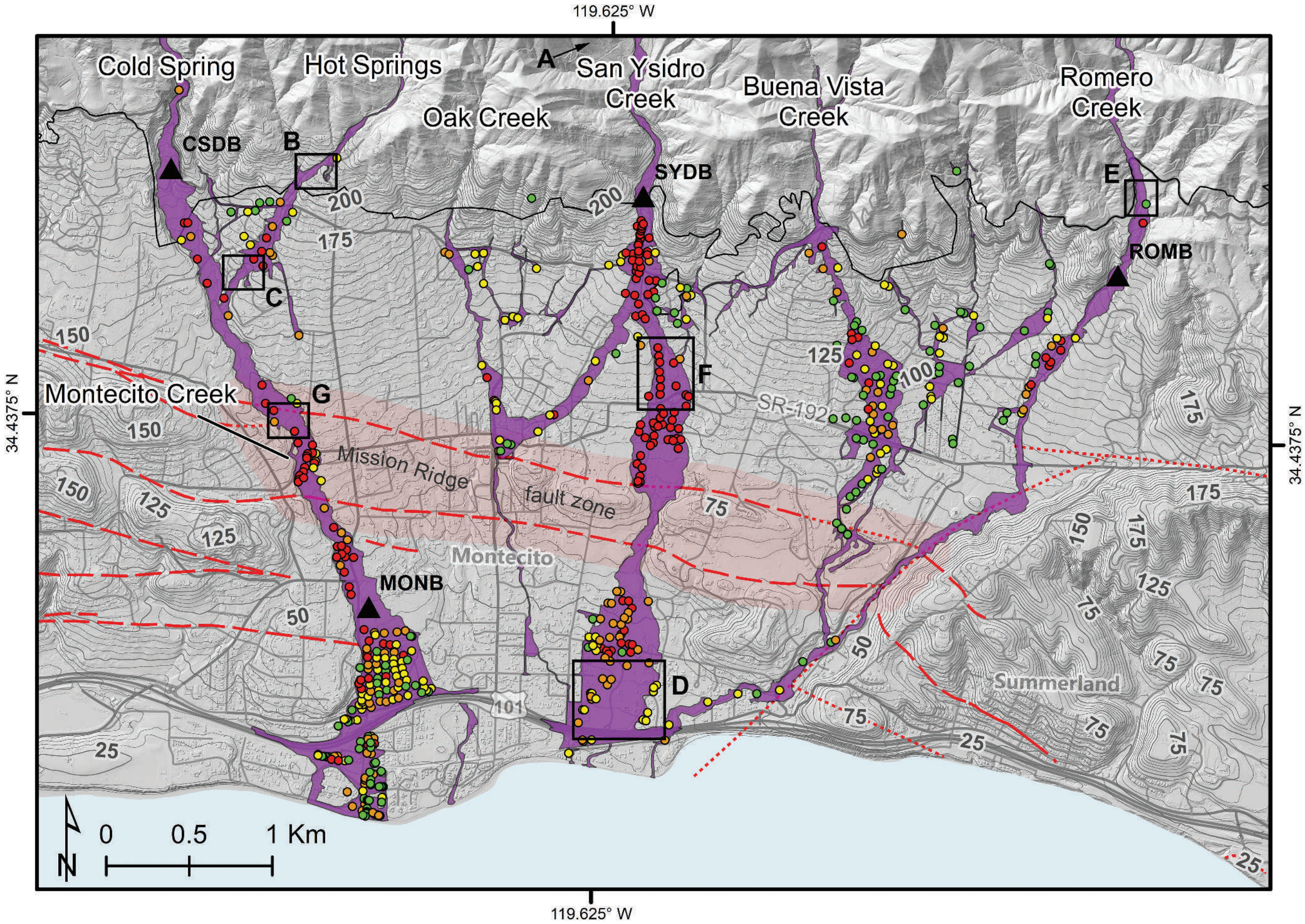

Figure 6. Topography and hillshade map derived from 1-m-resolution light detection and ranging (LiDAR) data of the Montecito area showing inundation in purple. Radial contours (in meters) indicate the presence of alluvial fans. The interaction of surge fronts with bridges, culverts, and roads on alluvial fans is apparent by the numerous large and small avulsions creating the distributary flow paths occupying roads and drainages. Mission Ridge Fault Zone is depicted as pink area across the middle portion of the piedmont; note: this is not a regulatory
3 fault zone (fault data from CGS, 2005). Other red lines depict faults, solid where accurately located, dashed where inferred, dotted where concealed. Names of canyons are in black with white outline, and the abbreviations for the debris retention basins (debris basins) are in black. Debris basin abbreviations: CSDB = Cold Spring; MONB = Montecito; SYDB = San Ysidro; ROMB = Romero. Damaged structures are shown as colored points from DINS data set (CAL FIRE, 2018b), representing state of damage as identified by the CAL FIRE–led damage assessment team: green = slight; yellow = moderate; orange = high; red = destroyed. Inset rectangles and numbers are keyed to Figure 10.

storms causing substantial damages in one area while completely bypassing another (USACE, 1999).

The 9 November 1964 post-fire storm event on the Coyote burn area caused flooding and debris flows within Montecito and San Ysidro creeks, resulting in approximately $500,000 in damages (in 1964 dollars; USACE, 1974, 1999). To the west, a debris flow destroyed 12 homes and six bridges on Mission Creek in Santa Barbara (Burns, 2018). Eyewitnesses reported 20-ft-tall (6.1 m) walls of debris moving down the affected channels at approximately 4.6 m/s (USACE, 1974).

On 25 January 1969, a winter storm impacted areas recovering from the 1964 Coyote Fire, flooding a large portion of Carpinteria and causing debris flows within the major tributaries of Montecito Creek (SBCFCD, 1969). Debris flows along Romero Creek avulsed from the stream channel just north of State Route 192 (SR 192), resulting in downstream flooding, including over U.S. 101. Approximately 100 homes in Montecito, and 250 homes and 20 commercial structures in Carpinteria were damaged as a result.

A 40 minute period of heavy rain on 27 December 1971 initiated flooding and debris flows carrying heavy loads of debris and mud in Romero, Garapata, Toro Canyon, Santa Monica, Franklin, and Carpinteria creeks, originating from watersheds that had been burned in the Romero Fire earlier that year (NOAA, 1971; CADWR, 1973). U.S. 101 near Carpinteria was blocked for 8 hours after a 3 ft (0.91 m) wall of mud

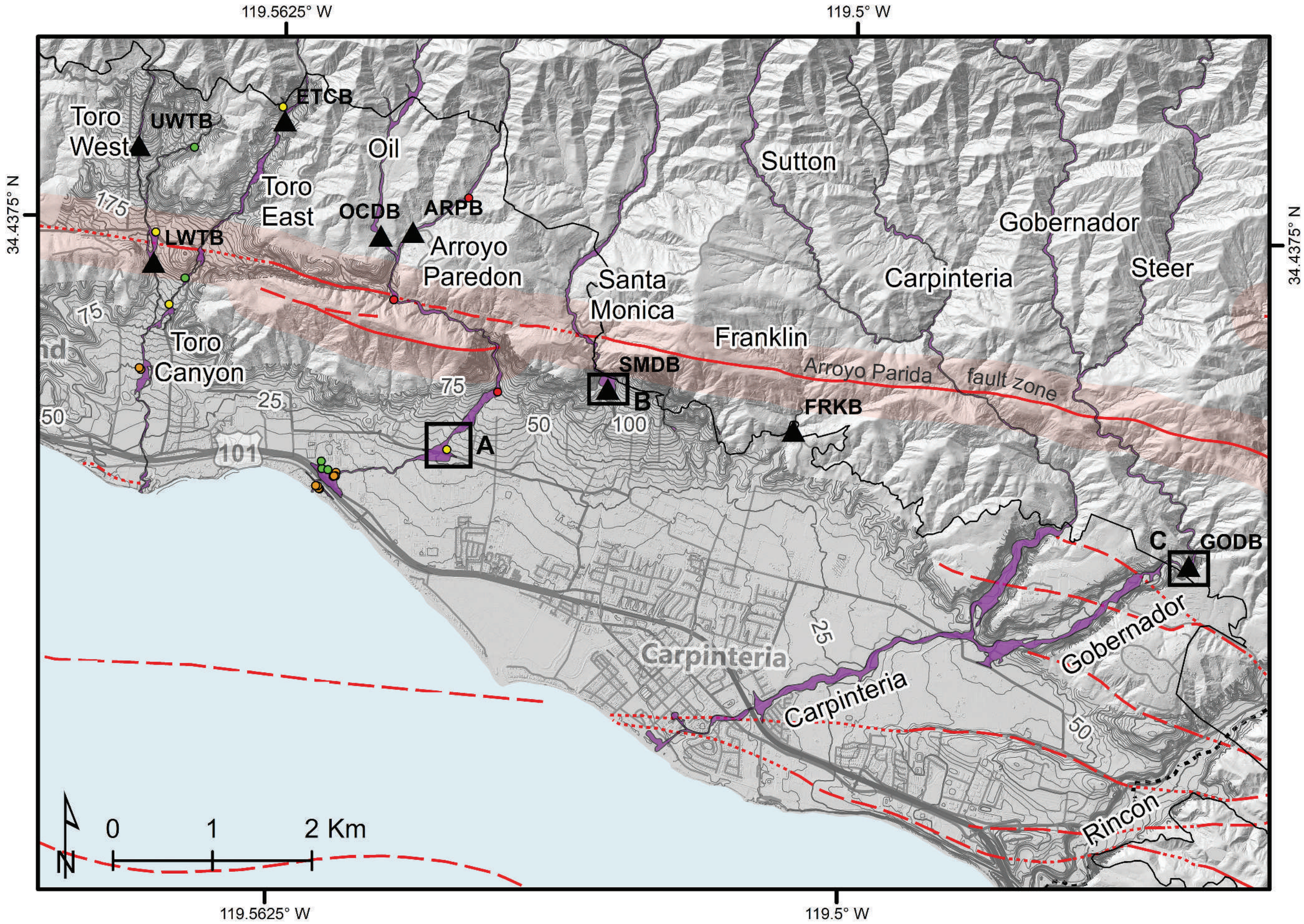

Figure 7. Topography and hillshade map of the Summerland and Carpinteria area showing inundation in purple. Radial contours (in meters) indicate the presence of alluvial fans that appear steeper, prominent, and active between Toro and Santa Monica canyons, and gently sloping, less prominent, and incised between Franklin and Carpinteria creeks. The Arroyo Parida fault zone is depicted as a pink area traversing the lower portion of the Santa Ynez Mountains; note: this is not a regulatory fault zone (fault data from USGS, 2019). Other red lines depict faults, solid where accurately located, dashed where inferred, dotted where concealed. Debris basin abbreviations: UWTB = upper west Toro; LWTB = lower west Toro ETCB = east Toro; OCDB = Oil Canyon; ARPB = Arroyo Paredon; SMDB = Santa Monica; FRKB = Franklin; GODBD = Gobernador. Damaged structures are shown as colored points from CAL FIRE DINS data set, representing state of damage as identified by the CAL FIRE–led damage assessment team: green = slight; yellow = moderate; orange = high; red = destroyed. According to the data set, no damaged private structures were mapped east of Arroyo Paredon. Inset rectangles and numbers are keyed to Figure 12.

and water pushed across it toward the ocean. Several roads and bridges were blocked and damaged. In the Carpinteria area, approximately 10–15 families were evacuated, and their homes were damaged, but no deaths or serious injuries occurred. Photos of Toro Canyon Park indicate the presence of boulder fields and woody debris, suggesting debris flows occurred in this event (USACE, 1974).

Prehistoric debris flows have been documented based on surficial deposits in the Santa Barbara and Montecito areas. These include a sequence of debris flows thought to be as old as 90–130 ky, a series in Rattlesnake Canyon thought to be 8 to 30 ky, a debris-flow deposit at Rocky Nook Park thought to be 1 ky, and a younger event in Rattlesnake Canyon thought to be less than 500 years before present (Keller et al., 2020a). While these surficial and stratigraphic prehistoric debris-flow data help to frame minimum recurrence intervals, stratigraphic records are often incomplete due to changes in loci of deposition and erosion in the fan environment (Coe et al., 2003; Wagner et al., 2012).

THE 9 JANUARY 2018 EVENT

During the storm, debris flows issued from numerous watersheds within the Santa Ynez Mountains (Figures 6 and 7). The first report of debris flows was a 911 call received at 3:47 am (PST) for an explosion resulting from debris-flow impacts to a gas

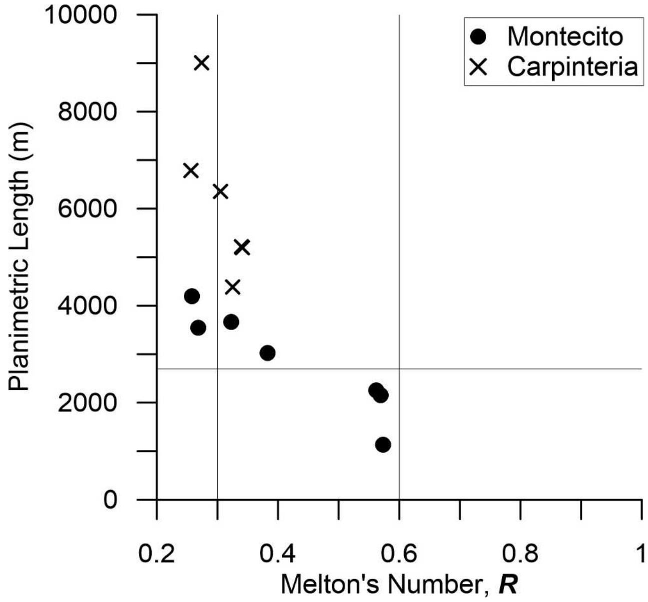

Figure 8. Plot of watershed planimetric length vs. Melton's number for watersheds north of Montecito and Carpinteria. Horizontal gray line is equal to a planimetric length of 2.7 km. Watersheds having a Melton's number falling between 0.3 and 0.6, with a planimetric length of <2.7 km, fall into the debris-flood category developed for non-fire settings. All of the data fall within the maximum and minimum values corresponding to post-fire debris-flow events documented in Gartner et al. (2014).

line buried below San Ysidro Creek. A security video camera showed that the debris flow reached a back yard on upper Cold Spring Creek at 3:49 am (Kean et al., 2019). Within the Montecito and Carpinteria areas, the debris flows continued past the canyon mouths and inundated portions of adjacent urbanized alluvial-fan surfaces and abandoned channels. In some locations, debris flows traveled up to 5 km to the Pacific Ocean. Of the destroyed structures, 79 had complete structural damage, including 41 structures that were swept off their foundations (Kean et al., 2019). Debris accumulated in low sections of U.S. 101, a major transportation corridor, rendering the section through Montecito impassable by vehicle for 13 days. Between 9 January and 22 January 2018, first-responder personnel conducted search and rescue operations, during which approximately 1,300 individuals were evacuated, and 700 sheltered-in-place (SBC, 2018a, 2018b). The Thomas Fire Presidential Disaster Declaration was amended on 10 January 2018 to include flooding, mudflows, and debris flows.

Meteorological Observations

A weak atmospheric river was present at the time of the event, demonstrating that catastrophic hydrologic impacts can occur even in the absence of substantial water vapor transport (i.e., a strong atmospheric river) due to synoptic-to-mesoscale forcing. Observations suggest that an NCFR (a narrow band of high-intensity rainfall in the vicinity of the cold front) and, to a lesser extent, orographic forcing produced the high-intensity rainfall in this event, with the weak atmospheric river serving as a moisture source (Oakley et al., 2018).

At approximately 1:00 am PST on 9 January, the north-to-south–oriented cold front was located just offshore of Point Conception and was propagating eastward across the southern California Bight. Radar imagery revealed the characteristic intense rainfall cores and lighter rainfall gaps of an NCFR parallel to the cold front (Figure 9). The NCFR impacted Montecito and Carpinteria beginning around 3:45 am PST and then began to dissipate near the Santa Barbara–Ventura County line around 4:18 am PST (Figure 9). The subsequent weakening of rainfall intensity likely spared other portions of the burn area from additional catastrophic debris flows.

Precipitation in this event was extreme at the 5 and 15 minute durations, with three locations recording >13 mm in 5 minutes, and several records were set at a few stations with 50+ years of observations (Oakley et al., 2018). Several stations demonstrated notable differences in the average return interval for these two durations. Triggering rainfall amounts at the 15 minute duration were as high as 26.16 mm in the Montecito area (Doulton Tunnel gauge) and 21.84 mm in Carpinteria (Carpinteria FS gauge), corresponding to return intervals of 50 to 100 years (Oakley et al., 2018). The Montecito station reported a 200 year precipitation event of 13.72 mm at the 5 minute duration and a 100 year event of 18.54 mm at the 15 minute duration (Oakley et al., 2018; SBCFCD, 2018).

Field Observations and Mapping

Methodology

Field observations, including documentation of debris-flow runout, area, and depth, are often used to classify debris-flow magnitudes and calibrate debris-flow models, and thus they were a primary consideration in our assessment (Hungr et al., 2007; Cannon et al., 2010; Scheidl and Rickenmann, 2010; Kean et al., 2011; Gartner et al., 2014; and Iverson, 2014). The distribution, characteristics, and source-area conditions of the debris flows were documented during three phases. The first "event response" phase was completed as a collaboration between the USGS and the CGS in the first 12 days after the event, documenting perishable features in the Montecito inundation area at 1,584 stations (Kean et al., 2019). The second

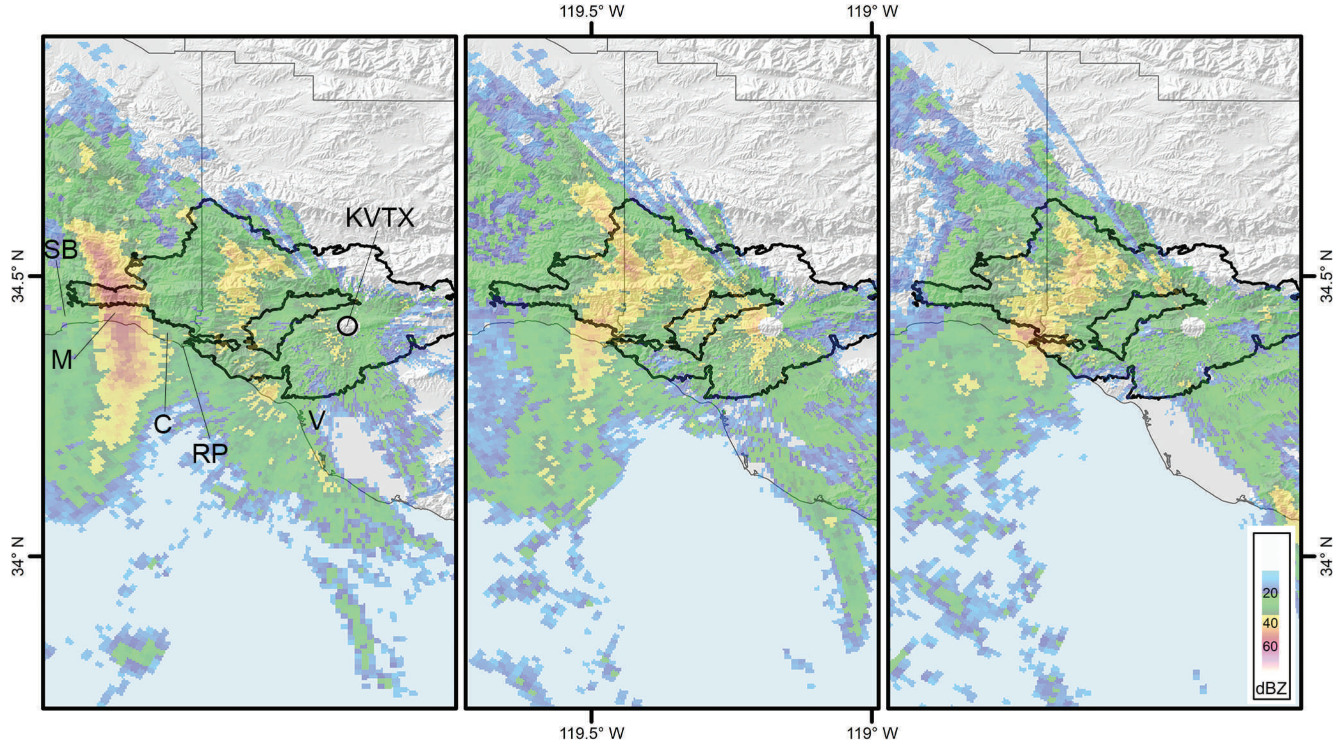

Figure 9. National Weather Service radar showing (A) the NCFR impacting the western portion of the Thomas Fire burn area at 3:45 am PST, 9 January 2018; (B) NCFR impacting the Summerland and western Carpinteria area at 4:07 am PST; and (C) NCFR breaking up at 4:18 am PST as it crosses the Santa Barbara and Ventura County line as it moved east. Annotations on left frame are Santa Barbara (SB), Montecito (M), Carpinteria (C), Santa Barbara County line at Rincon Point (RP), Ventura (V), and the National Weather Service Radar location (KVTX). Data are from: https://www.cnrfc.noaa.gov/radarArchive.php.

phase consisted of field mapping debris-flow source areas and channel conditions from Montecito to Rincon Creek at 458 stations. Phase three consisted of assessing the extent of debris-flow initiation and inundation across the remainder of the Thomas Fire area, establishing triggering rainfall amounts, and refining damage and cost data from Lukashov et al. (2019). In all phases, field observation data on debris-flow occurrence, scour depth, maximum flow depth, channel gradients, peak flow heights, and super-elevation were collected in the channel areas; field observation data on geometry and extent of rills, sheet-flow erosion, micro-levees, inter-rill areas, soil depth, slope gradient, and slope geometry were collected in hillslope areas above Montecito.

Montecito Area

Hillslopes

Hillslopes are generally underlain by three primary material types with respect to erosion characteristics, which correspond to Maymen-Rock Outcrop Complex soils (either 75–100 percent or 50–75 percent slopes). These include: (1) steep slopes (>75 percent or 36.9°) dominated by rock outcrops that are underlain primarily by resistant sandstone beds of the Coldwater or Matilija formations; (2) slopes mantled by angular to subangular, cobble- to boulder-size rocky debris, where this debris was derived from underlying weathered sandstone beds of the Coldwater or Matilija formations, sandstone interbeds of the Juncal Formation or Cozy Dell Shale, or secondary debris-fan and colluvial deposits; and (3) moderately steep slopes (47 to 75 percent or 25° to 37°) underlain by dominantly fine-grained sections of the Juncal Formation and Cozy Dell Shale, which commonly form more geomorphically uniform slopes with a thin mantle of soil.

Slopes Underlain by Rock Outcrops—Surface runoff on slopes underlain by rock outcrops coalesced into intervening gullies that were typically scoured of loose debris in the upper reaches, exposing either bedrock or consolidated gravelly soils. In the lower reaches, the gullies either fed into larger channels, or they conveyed the scoured debris through rocky colluvial deposits or small fan deposits, sometimes leaving rocky levee deposits above the channel banks.

Slopes Mantled by Rocky Debris—On rocky slopes, runoff was observed either to flow around the clasts, scouring away much on the intervening finer debris, or to form coarse, meandering rills. The majority of cobble and larger size clasts on rocky slopes did not appear to have moved much during the debris-flow event. This lack of mobilization suggests that nearly all of the large debris (boulders) observed in the inundation zone was entrained from existing coarse deposits within the channel areas.

Slopes Underlain by Fine-Grained Bedrock—Slopes underlain by fine-grained bedrock typically exhibited varying degrees of rill (discrete flow paths) or sheet-flow erosion, depending on the soil thickness, slope gradient, and slope geometry (Figure 10A). Rill geometry varied depending on whether the plan-form slope geometry was convex (divergent), concave (convergent), or planar. Rill and/or sheet erosion began just a short distance below the ridgelines. The proportion (area) of slopes displaying rills or sheet flow typically increased with slope gradient, and the width of erosion paths commonly increased where the gradient increased downslope.

The depth of erosion typically varied with the original depth of soil that was disaggregated by heating during the fire, which was controlled in part by original soil thickness and soil burn severity, and hence by slope gradient and pre-fire vegetation density. Soils remaining below the disaggregated layer were typically more cohesive and contained fine roots, which impeded erosion during the heavy but brief rain event. On some heavily eroded slopes, rills scoured below the disaggregated soils into low-cohesion soils with fine/small roots. Rill depth only increased slightly downslope on planar or divergent slopes. However, rill depths did increase on convergent slopes and swales, where rills merged downslope to form deeper rills and gullies, or where slope gradient decreased and/or the depth of loose soil increased downslope, commonly resulting in deeper, narrower, more meandering rills. The cross-sectional area of rills did commonly increase downslope on all slope types, primarily reflecting the development of wider rills in the loose, disaggregated soils, as noted in Keller et al. (2020b). Rill and inter-rill dimensions were recorded at six, 30-m-long transects located on soils of the Juncal Formation in the upper reaches of Cold Spring and San Ysidro canyons on slope gradients ranging from 17° to 37°. The ratios of rill width to maximum depth are summarized in Figure 11. The percent of slope eroded ranged from 51 to 83 percent, although the presence of concentrated gravel mantling inter-rill areas suggests that some finer soils were also winnowed away between rills. Median width-to-depth ratios ranged from about 8 to 13, with median rill widths ranging from 50 to 100 cm and median rill depths ranging from 4 to 10 cm at each transect.

Micro-levees were locally observed along the margins of rill and sheet-flow paths. Micro-levees appeared to be most common where soils were thicker and/or where slope gradients decreased downslope; micro-levees were typically less than 10 cm in height in gravelly and sandy soils, but they locally ranged up to about 20 cm high along the larger rills and gullies.

Observation of soils in unburned areas indicated that little to no rilling or other erosion occurred under the vegetation canopy during the rainfall event and that gravel was commonly present in the soil profile, but gravel pavement was not well developed in comparison with inter-rill areas in the burn area. Natural hydrophobicity was observed where tested at the base of the shallow organic horizon in these unburned areas.

Source Channels

The maximum depth of inundation during the debris-flow event was recorded at several stations in each of the subject canyons north of Montecito. In the two largest canyons (Cold Spring and San Ysidro), inundation depths ranged up to about 10 m in the lower reaches and generally decreased upstream into the headwaters; however, greater inundation depths of up to 14.7 m were locally observed where channel constrictions or bends caused super-elevated conditions. In the smaller drainages, inundation depths reached observed maxima of 9.3 m in Romero Canyon, 6.4 m in Hot Springs Canyon, and 6.2 m in Buena Vista Canyon (Table 2). The source channels were dominated by transport and scour processes with overbank deposits preserved on localized inset alluvial surfaces as thin drapes of sandy mud and gravel up to 20 cm thick and boulders stranded against trees or other obstacles. Scour depths typically ranged from 0.5 to 2.0 m with an observed maximum of 3.0 m, and exposed bedrock along more constricted reaches (Figure 10E). Trees surviving in the flow path were marked by mud patinas and scarring, which helped to define flow depths. Evidence of significant past historic flows includes healing tree scars in Romero Canyon and pre-event overbank boulder deposits and levees in Hot Springs Canyon. Older debris-flow deposits were widely observed in channel banks, and pre-event levees were found at many locations above the channel banks.

Debris Basins

Constructed debris-retention basins (debris basins) present at the time of the 9 January debris flow included basins at Cold Spring, San Ysidro, and Romero canyons, and on Montecito Creek (Figure 4). All of these basins were reportedly cleared of debris prior to

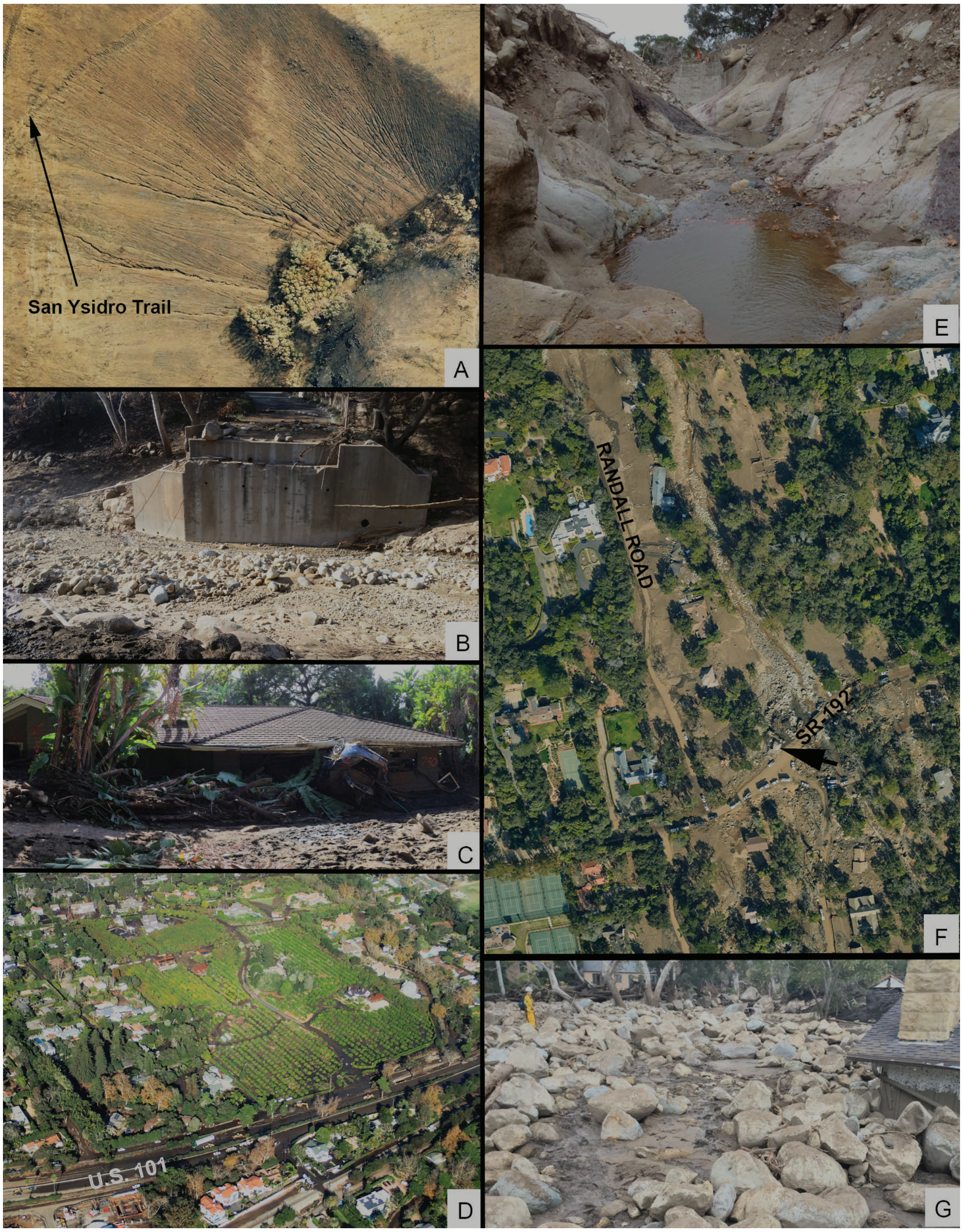

Figure 10. Photo locations from inset rectangles on Figure 4. (A) Aerial photo showing deep rills and gullies in soils formed on shale and siltstone beds (Tj on geologic map), where eroded U.S. Forest Service San Ysidro Trail on hillslope is roughly 1.5 m in width (San Ysidro Canyon, north is up). (B) View west toward bridge deck knocked off abutments by debris-flow surge front on Hot Springs Creek; note: boulder remnant on left side of abutment were stranded after surge front removed deck. (C) View south of car jammed into home on Hot Springs Creek. (D) View northeast of lower piedmont gently sloping streamflow fan with broad fine-grained debris deposition through citrus orchards and U.S. 101 to the south. (E) View south of channel alluvium scoured down to moderately cemented Coldwater Sandstone bedrock (Tcw on geologic map) on upper Romero Creek; note: cobble-boulder alluvium from past debris flows mantling Tcw bedrock. (F) Aerial photo of San Ysidro Creek on the east side and running north-south and parallel to Randall Road, where numerous homes were destroyed or swept away; San Ysidro Creek crosses East Valley Road (SR 192) in the lower right side of the photo, and arrow points to boulder having a maximum diameter of about 6 m. (G) View of boulder debris field indicating surge-front deposition up to eves of a home located on Montecito Creek.

Table 2. *Montecito inundation data based on field observations and mapping, modified from Kean et al. (2019). Runout distance was taken as the full length of the flow path on which debris flows were observed. Surge-front distances were taken from the topographic break at the mountain front to the first and last series of boulder fields deposited in the creeks and on the alluvial fans, as interpreted from observations in this study and described in Kean et al. (2019). Maximum inundation depths represent confined channels rather than overbank areas observed after the event and do not consider channel modification by scour and transport due to the debris flows and subsequent clear-water recessional flows. A k value of 3 was used in the forced vortex equation to estimate debris-flow velocity.*

Channel Name	Runout Distance (km)	Runout of Boulder Surge-Front Deposition (km)	Maximum Depth (m) and Velocity (m/s) in Canyon	Maximum Depth (m) and Velocity (m/s) on Fan	Maximum Boulder Dimension on Piedmont (m)
Montecito	4.2	0.5–2.5	NA/NA	10.0/NA	4.8
Cold Spring	NA	NA	10.1/6.4	NA/NA	4.8
Hot Springs	NA	NA	6.4/4.7	NA/NA	2.2
Oak Creek	1.8	0.15–1.0	1.5/NA	3.0/3.0	1.2
San Ysidro	4.2	0.75–1.45	14.7/6.4	7.0/2.5	6.0
Buena Vista	4.4	0.0–0.7	4.6/5.4	5.4/NA	3.0
Romero	5.0	0.0–1.4	9.3/6.6	7.0/4.0	2.1

NA = not applicable.

the storm, but they were filled to capacity and overtopped by debris during the 9 January debris-flow event.

Inundation Zone

The debris-flow inundation covered an area of 3.15 km^2, and flows from individual canyons reached the ocean up to 5.0 km from the mountain front (Table 2). Surge-front depths in the upland canyons ranged from 1.5 to 14.7 m in the confined canyons to 3 to 10 m on the piedmont. Trunk channels acted as primary conduits of the event flows, but flows were commonly at or above the capacity of previously existing channel banks and overflowed onto elevated alluvial-fan or terrace surfaces bordering the trunk channels (Figures 6 and 10). Overbank flows and avulsions occurred at channel constrictions, including culverts, bridges, and associated bridge abutments (Figure 10B), and outer banks of channel bends, where the phenomenon of super-elevation generated increased debris-flow height. Overbank flows inundated adjacent fan surfaces and opportunistically occupied roads and dormant distributary channels (Figures 6, 10D and F). Prominent avulsions occurred at Buena Vista Creek, at Lilac Drive and Alisos Drive, San Ysidro Creek at Randall Road, at U.S. 101 from both San Ysidro and Montecito creeks, and at Oak Creek north of San Ysidro Road (Figure 6). Channels were generally pathways of debris transport and variable scour with local deposition upstream of choke points, while overbank surfaces were dominantly areas of transport and deposition. The maximum inundation elevation on alluvial surfaces was consistently higher than the final surface elevation of deposits left after the event due to the passing of elevated surge fronts and dewatering of deposits.

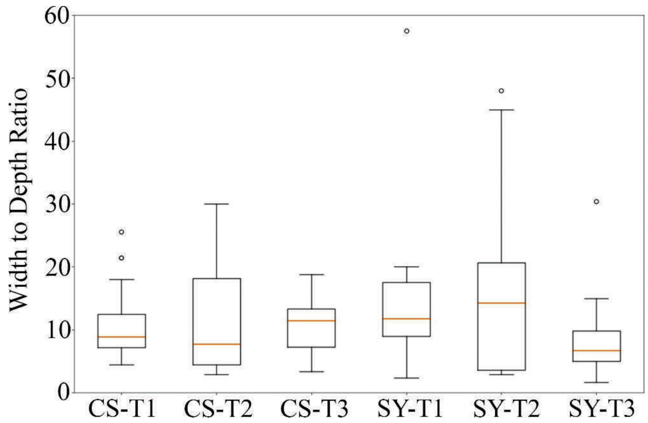

Figure 11. Box-and-whisker plots showing width-to-depth ratios of hillslope rills based on hillslope erosion transects in Cold Spring and San Ysidro canyons. Central orange line is median of data, and upper and lower limits of box are defined by 25th and 75th percentiles; whiskers illustrate upper and lower quartiles, and dots represent statistical outliers. All transects were measured in the Juncal Formation, corresponding to Maymen-Rock Outcrop Complex soil series on generally planar to slightly convex slopes in plan curvature (CAL FIRE, 2018). Plot locations are CS-T1: 34.4880°N, 119.6664°W; CS-T2: 34.4854°N, 119.6554°W; CS-T3: 34.4733°N, 119.6393°W; SY-T1: 34.4718°N, 119.6015°W; SY-T2: 34.4708°N, 119.6021°W; SY-T3: 34.4709°N, 119.6070°W. Data were originally plotted by Francis Rengers, USGS.

4

Debris-flow deposits observed on inundated surfaces were typically bimodal. The fines fraction consisted of dark-gray, muddy sand with ash and variable gravel content; gravel content diminished with increasing distance from the mountain front; laboratory testing of debris-flow matrix samples indicated a classification of silty sand (SM) per the Unified Soil Classification System (Kean et al., 2019). The coarse fraction consisted of small to large boulders, up to a maximum documented diameter of 6 m; larger boulders may have been captured in the debris basins, but the dimensions of boulders removed from the basins were not systematically documented. Cobble-size clasts were conspicuously uncommon among the surface deposits, but they may have been more plentiful buried within the debris basins.

Boulders composed of strongly indurated sandstone derived primarily from the Matilija and Coldwater formations were deposited on alluvial surfaces and channel banks, accumulating as levees, boulder fields, stacked rocks, or isolated rocks in more distal areas (Figure 10F and G) and providing evidence of surge-front deposition. Boulders were subangular to subrounded and oblong to tabular in shape. Large boulder field deposits were concentrated at the confluence of Cold Spring and Hot Springs canyons, north of SR 192, near Hot Springs Road along Montecito Creek, and along San Ysidro Creek both north and south of SR 192, including Randall Road (Figure 10F). Less concentrated boulder deposits were observed elsewhere along these creeks down to San Benito Way along Montecito Creek and down to San Leandro Way along San Ysidro Creek. Boulder deposits were also observed along Buena Vista Canyon north of SR 192, and sporadically along the upper reaches of Romero Canyon and below the confluence of Romero and Picay creeks.

Summerland and Carpinteria

Source Channels

Slope conditions in the upper reaches of the canyons east of Montecito were not observed in detail in the field during this study owing to limitations on time and access. However, review of imagery and light detection and ranging (LiDAR) data indicate that extensive rilling and erosion occurred during the 9 January storm, similar to the canyons north of Montecito. Field observations and imagery indicate that debris flows formed in each of the canyons as well; however, the down-canyon extent of the flows decreased from west to east. This in part reflects decreasing rain intensity as the rain band dissipated to the east, the increasing length of the trunk drainages to the east, and smaller proportions of watershed burned. The longer drainages at lower gradient allowed more coarse debris to drop out of the flows and transition into hyperconcentrated flows or flood flows downstream. Inundation depths up to 6.7 m were locally observed where channel constrictions or bends caused super-elevated conditions (Table 3).

Debris Basins

Constructed debris basins are present on Toro Canyon east, Toro Canyon west (upper and lower), Oil Canyon and Arroyo Paredon (north of the confluence with Oil Canyon), Santa Monica Canyon, Franklin Creek, and Gobernador Creek (Figures 7, 12B and C). These debris basins, except for Oil Canyon, which has not been maintained, were reportedly cleared of debris prior to the event. Debris flows tested or exceeded the capacity of all the debris basins except the lower west Toro, Franklin, and Santa Monica basins. Farther east at Gobernador Canyon, bouldery debris mostly settled out within the upper portion of the broad, unconfined basin footprint (Fig 12C), but flood flows carried large woody debris over the bollards, much of which accumulated against bridges downstream.

Inundation Zone

Substantial debris flows and sediment-laden flows occurred in all of these canyons except Rincon Creek (Figure 7), with inundation covering an area of 2.41 km^2. Surge-front depths ranged from 5.0 to 6.9 m in the confined canyons to 1.2 to 5 m on the piedmont (Table 3). Out-of-channel flow and inundation of structures due to avulsion were less extensive than in the Montecito area, and none resulted in fatalities. The only gauged runoff in the entire coastal plain was recorded in Carpinteria Creek at Casitas Pass Road, with a maximum discharge at 4:45 am PST reaching a reported stage height of 16.7 ft (5.0 m) and initially a peak discharge of about 15,000 ft^3/s (424.8 m^3/s), which is currently under review (USGS Gauge ID# 11119500) (Laber, 2018). This was roughly 40 minutes after the peak 5 minute duration rainfall was recorded at the Carpinteria rain gauge. Wood- and sediment-laden surge fronts were conveyed for 2.4 km in Carpinteria Creek and deposited at U.S. 101 and Carpinteria Avenue.

Debris-flow inundation occurred due to numerous avulsions along the lower portion of the piedmont south of Toro Canyon (Figure 7). Farther east, a debris-flow avulsion occurred on an inset alluvial surface of the Arroyo Paredon fan (Figure 12A). At the location of the apex avulsion, additional boulder debris was deposited and backfilled the previously entrenched fan head; downstream, additional boulders and woody debris were deposited against the bridge crossing at Foothill Road (SR 192), and this constriction enhanced avulsions into adjacent downstream areas. Flows that reached the frontage road (Via Real) north of U.S. 101 were mostly muddy with woody debris. Farther east at Santa Monica, Franklin, and Carpinteria creeks, flows were contained near the

Table 3. *Summerland and Carpinteria inundation data based on field observations and mapping. Runout distance was taken as the full length of the flow path on which debris flows were observed. Surge-front distances were taken from the topographic break at the mountain front to the first and last series of boulder fields deposited in the creeks and on the alluvial fans, as interpreted from observations. A value of zero for runout distance indicates that debris flows did not travel beyond the fan apex or topographic break at the mountain front. Significant flows of finer-grained sediment and woody debris discharged from spillways at both the Santa Monica and Franklin debris-retention basins. These flows were deposited in the Carpinteria Salt Marsh Preserve.*

Channel Name	Runout Distance (km)	Apparent Boulder Surge-Front Deposition (km)	Maximum Depth (m) and Velocity (m/s) in Canyon	Maximum Depth (m) and Velocity (m/s) on Fan	Maximum Boulder Dimension on Piedmont (m)
Toro	4.0	0.0–1.0	5.0/5.7	3.5/3.3	3.0
Arroyo Paredon	2.6	0.0–0.8	4.3/NA	3.0/NA	3.9
Santa Monica	0.0	Debris basin	6.7/4.2	1.2/NA	NA/NA
Franklin	0.0	Debris basin	NA/NA	NA/NA	NA/NA
Carpinteria	3.4	In canyon	NA/NA	5.0*/NA	3.0
Gobernador	NA	Debris basin	4.0/5.0	4.7/4.5	3.0
Rincon	0.0	No debris flow	No debris flow	2.3/NA	NA/NA

NA = not applicable.
*Depth from Carpinteria Creek is from USGS gauge record.

mountain front by debris basins, and outflows below the mountain front consisted of primarily fine-grained sediment and woody debris with scattered boulders.

Debris-Flow Volume and Magnitude

The total volume of debris generated by flows in the Santa Barbara Coastal Plain is estimated at 1,498,000 m^3. This volume includes the reported total volume of 260,342 m^3 of debris removed from debris basins (SBCFCD, 2018) and 126,008 m^3 removed from creek channels (USACE, 2018), but it does not include the volumes of debris removed from U.S. 101, or the volumes that reached the ocean, which were not directly documented. In addition, sediment thicknesses recorded at 373 post-event field stations were used to estimate debris volume distributed over inundated areas in Montecito and Summerland. The total mapped inundation area is 5,560,000 m^2 (revised from Lukashov et al., 2019), and the average deposit depth is 0.3 m with a standard deviation of 0.53 m. Because the data do not have a normal distribution and are heavily skewed by large outliers, a median thickness of 0.2 m was adopted (Schiff and D'Agostino, 1996), which gives an estimated deposited debris volume of 1,112,000 m^3.

Jakob (2005) classifies boulder debris flows in a volume-based logarithmic scale up to magnitude 6, where magnitudes 7–10 are used only for volcanic debris flows. However, the distributed nature of source areas combined with depositional overlap of debris-flow deposits restrict the ability to separate material by watershed as used in Jakob (2005), so they are considered here as an aggregate event. The cumulative estimated volume for this event is greater than 1,498,000 m^3, and the aggregate inundation area is over double the value used for the magnitude 6; therefore, we classify the event as a magnitude 7 debris flow. In comparison, flows following the 1964 Coyote Fire and the 1971 Romero Fire each impacted an estimated area of greater than 2 km^2 for a magnitude 5 classification (Jakob, 2005; Lancaster, 2018).

Volumes of flows from individual canyons were poorly constrained because of the depositional overlap, and most debris basins were overwhelmed or lacking. Two exceptions were west Toro Canyon (upper and lower) and Santa Monica Canyon, where the basins were large enough to contain the debris-flow material. Using the empirical model of Gartner et al. (2014), mean volume estimates of 40,681 and 100,437 m^3 were developed using 40 mm/hr rainfall intensity at west Toro Canyon and Santa Monica Canyon, respectively (Table 4). The rainfall intensity documented near these canyons was between 79.24 and 104.64 mm/hr (Oakley at al., 2018). The observed volume was 53 percent of the predicted volume at west Toro and 119 percent of the predicted volume at Santa Monica, which are within the standard deviation reported by the USGS.

Large amounts of riparian woody debris were scoured from channel networks and transported into the built environment, creating debris dams at culverts and bridges. The quantity of woody debris is unknown and cannot reliably be taken as a percentage of the total volumes presented, as woody debris was largely absent from the overtopped debris basins, and was not disseminated among the debris-flow deposits, but rather formed piles and rack deposits against structures, trees, and other obstacles.

Table 4. *Debris basin removal volumes compared with USGS mean debris-flow volume estimates using empirical equations from Gartner et al. (2014) and the maximum rainfall intensity input in the model. Percent of USGS predicted volume was calculated between clean-out volume and the predicted volume. "Greater than" symbol denotes where debris flows filled and overtopped the debris basin, and thus locations where the removed volume accounts for a part of the volume that inundated downstream areas.*

Debris Basin[*]	Construction Year	Removal Volume[†] (cm)	Capacity Exceeded or Contained	USGS Mean Volume (cm) at 40 mm/hr[†]	Percent of USGS Predicted Volume
Cold Spring	1964 (USACE)	18,947	Exceeded	60,207	>32%
San Ysidro	1964 (USACE)	16,627	Exceeded	84,883	>20%
Romero	1971 (USACE)	33,041	Exceeded	45,387	>73%
W Toro Upper & Lower	1971 (USACE)	21,555	Contained	40,681[‡]	53%
E Toro	1971 (USACE)	11,584	Exceeded	29,055	>40%
Arroyo Paredon	1971 (USACE)	18,371	Exceeded	43,012	>43%
Santa Monica	1977 (USDA)	119,271	Contained	100,437[‡]	119%
Franklin	1971 (USACE)	888	Contained	14,309	6%
Gobernador[§]	1971/2008	8,722	Contained	240,303	4%

[*]Most basins were constructed with grouted boulder dam and culvert; Montecito debris basin volume (1,778 cm) and Plunge Pool volume (9,557 cm) not included.
[†]Volume of debris removed after January 9 event, as reported by USACE.
[‡]USGS mean volume compiled from multiple contributing sub-watersheds.
[§]Gobernador was originally constructed in 1971 with 25,275 cubic yard (19,324 m^3) capacity, and then it was modified in 2008 to allow fish passage.

Debris-Flow Velocities

Debris-flow velocity estimates were calculated from observations of super-elevation at 52 channel bend locations, expanding on the data set for Montecito summarized in Kean et al. (2019). The super-elevation, or the slope between the high- and low-flow marks of a debris flow around a curving channel, can be used to back-calculate and estimate velocity with the forced-vortex equation (Chow, 1959; Hungr et al., 1984; Prochaska et al., 2008; Kean et al., 2019); procedures described in Kean et al. (2019) were followed herein, including adoption of a k correction factor of 3. Estimated debris-flow velocities ranged from 4.2 to 6.6 m/s within the source canyons, and from 2.5 to 4.0 m/s on fan areas at Montecito, Summerland, and Carpinteria (see Tables 2 and 3). In addition, review of video footage of unconfined flows along Olive Mill Road (asphalt-concrete paved) from the lower portion of Montecito Creek revealed a velocity of 3.7 m/s, which is within the observed range of super-elevation velocities estimated elsewhere in fan areas.

Frequency

To develop quantitative hazard information, a focus on Holocene climate, anthropogenic climate change, historic and prehistoric data is needed (Jakob et al., 2017; Williams et al., 2019). Charcoal accumulation rates from marine sedimentary cores off the coast of Santa Barbara and documented historic wildfires indicate the average return period for large wildfires (>50,000 acres) is approximately 21 years for pre-European settlement periods, 29 years for the European settlement period, and 23 years for the 1900s (Byrne, 1979; Mensing et al., 1999). A review and statistical analysis of wildfires confined to the Santa Barbara Coastal Plain (from Gaviota Beach to the Ventura County line) suggest that from 1913 to 2017, more than 63 wildfires greater than 0.04 km^2 (10 acres) occurred in the region (CAL FIRE, 2018c; Lancaster, 2018). Using these wildfire data, a statistical analysis of wildfire return period suggests that the annual return period for a wildfire of 7.8 km^2 (2,500 acres) is about 2.7 years, an area slightly larger than the San Ysidro Creek watershed and similar in size to the El Capitan watershed that produced a PFDF on 20 January 2017 (Schwartz, 2017). Whereas the statistical return period equivalent to the area within coastal-draining portions of Santa Barbara County consumed by the Thomas Fire (89 km^2 or 22,000 acres) is about 10 years (Table 5).

Table 5. *Fire size and annual return period for the Santa Barbara Coastal Plain using fire-history data from CAL FIRE (2018) and analysis from Lancaster (2018).* 5

Fire Size (acres)	Annual Probability of Exceedance	Annual Return Period (years)
500	53.74	1.86
5,000	28.39	3.52
10,000	20.75	4.82
22,300	11.92	8.39
50,000	3.03	32.96

Figure 12. Photo locations from inset rectangles on Figure 5. (A) View north of Arroyo Paredon Creek north of Foothill Road, showing boulder fields from surge-front deposition in previously entrenched channel. Maximum boulder size observed in this general area was 3.9 m. (B) View south of Santa Monica debris basin (SMDB on map) full of fine-grained slurry with piles of racked trees and woody debris around the spillway; massive boulder field located with arrow and shown as inset photo indicates where some of the surge fronts came to rest as flow front lost both confinement and gradient (photo taken by Lael Wageneck, SBCFCD). (C) View north of Gobernador debris basin (GODB on map) with concrete breakers at the outlet, and boulder deposition from debris-flow surge fronts at the upstream junction of the creek and debris basin; largest boulders are 2.5 m in maximum dimension.

The historical frequency of both wildfire and triggering rainfall provides context to quantitative hazard assessments (Kean and Staley, 2019). Using the return intervals (RI) for rainfall intensity at the 15 minute duration for the 9 January storm rainfall (Perica et al., 2011; Oakley et al., 2018) and the fire frequency data presented in Table 5, the joint probability for debris flows being triggered in a single watershed, where joint probability equals P(A) × P(B), would be 0.0066 (150 year RI) and 0.0033 (300 year RI) for the 50 and 100 year storm event, respectively. The joint probability for debris flows being triggered in multiple watersheds at the scale of the Thomas Fire's footprint in Santa Barbara County would be 0.002 (500 yr RI) and 0.001 (1000 yr RI) for the 50 and 100 year storm event, respectively. Considering that debris flows in multiple watersheds occurred after wildfires in 1964, 1971, and 2018, an average return period for widespread damaging or catastrophic debris flows based on physical evidence may be less than 20 years. The difference in recurrence between coupled fire and triggering precipitation and historic PFDF data highlights the importance of a multi-faceted assessment approach, including a cumulative magnitude-frequency analysis, as suggested in Jakob et al. (2017).

DEBRIS-FLOW SOURCES AND RAINFALL

Sources of debris-flow material include residual and colluvial soils from steep slopes, and alluvial wash and valley deposits (Cannon et al., 2003; Santi et al., 2008). Hillslope sediment is entrained and delivered to channels by rilling and gullying that result from intense surface erosion during runoff. Research suggests that rills develop as micro-slope failures initiated by small slips at depth due to increases in pore pressure (e.g., Wells, 1987; Gabet, 2003). Within channel networks, debris-flow initiation is poorly understood. As with hillslope rill initiation, several researchers suggest that debris-flow initiation may result from mass failure of the channel bed or, alternatively, as a result of grain-by-grain entrainment and bulking by hydrodynamic forces from a critical discharge of water (e.g., Armanini and Gregoretti, 2005; Lamb et al., 2008; and Kean et al., 2013). Kean et al. (2013) examined the dynamics of debris flows as initiated by small sediment surges, which appear to result from low-gradient slopes temporarily storing sediment as "sediment capacitors." This dynamic includes minute slope failures, while still allowing inferences to be drawn about rain intensities needed to trigger different surge magnitudes (Kean et al., 2013). Once a debris flow is triggered, it gains mass from sediment bulking by scour and erosion in source areas and confined piedmont channels. Numerous researchers have attempted to quantify hillslope sediment contributions, finding that as little as 3 percent to as much as 93 percent of total debris comes from hillside erosion (Santi et al., 2008; Staley et al., 2014).

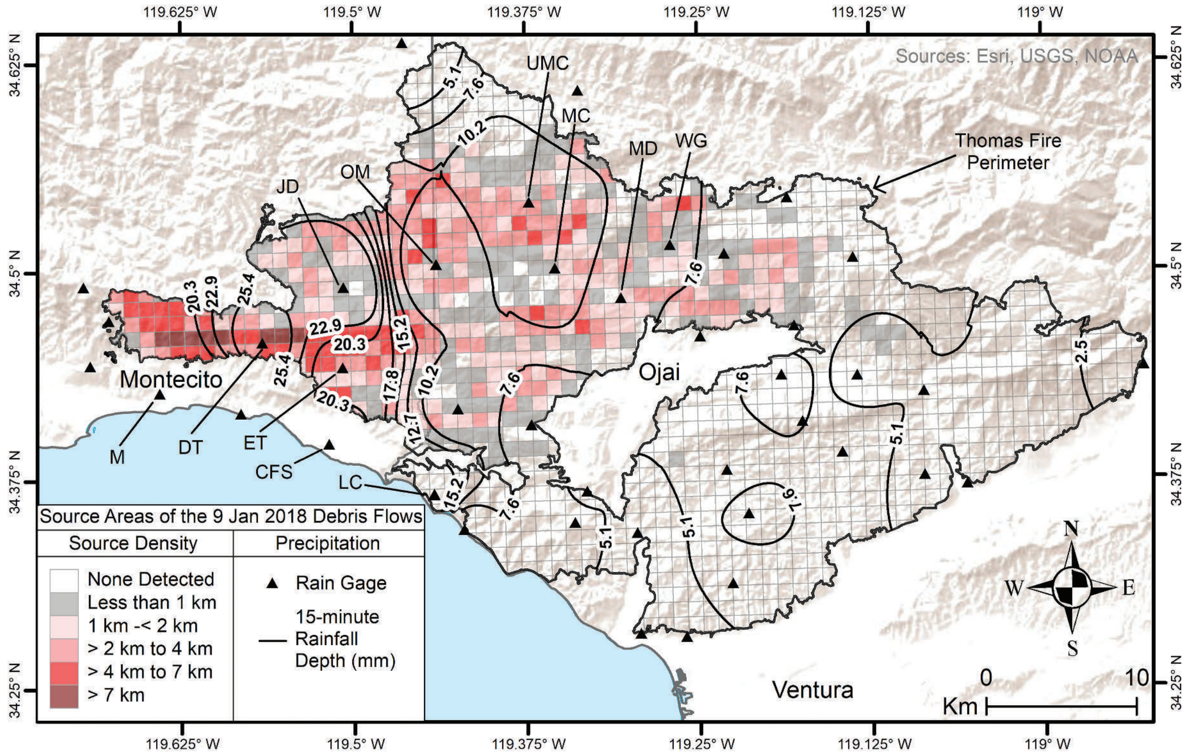

Figure 13. Maximum 15 minute rainfall amounts (mm) over a 1 km^2 grid representing the cumulative linear kilometers of debris-flow source gullies greater than 1.5 m in width; debris flows in gullies less than 1.5 m wide or those interpreted with questionable confidence, are not represented in this figure. The rain gauges within the burn perimeter annotated on this figure are summarized on Figure 14. Note: A portion within the northern-most burn perimeter in proximity to the county line and the northern-most gauge were mapped by the U.S. Forest Service as unburned based on the soil burn severity map (CAL FIRE, 2018), and thus post-fire debris-flow activity would not be expected. 6

Debris-flow source area mapping utilized (Lukashov et al., 2019) an interpretive and digitizing scale between 1:500 and 1:1,250, based on a systematic review of hillshade and aerial photos that were field validated at 184 sites and included a debris-flow confidence classification matrix following Wills et al. (2017). In total, 1,222.3 km of source gullies (≥1.5 m width) were mapped throughout the burn area. Approximately 600 km were mapped in Santa Barbara County and 620 km in Ventura County. Source gullies interpreted as definite were mapped with an accuracy of 98 percent, probable gullies had an accuracy of 69 percent, and questionable gullies had an accuracy of 22 percent. Debris-flow sources were intersected with a 1 km^2 grid, weighted by their confidence, and summarized for each grid cell (Figure 13).

Peak 15 minute rainfall amounts from the storm were collected from 46 gauges maintained by the Santa Barbara County Public Works Department and Ventura County Watershed Protection District. These amounts, irrespective of time, were plotted and interpolated with the inverse-weighted distance method in ArcGIS (Chen et al., 2017) and are shown in black on Figure 13. Furthermore, the rainfall depths are plotted against maximum source density data on Figure 14.

Corresponding to damaging impacts in Montecito, Figure 13 shows a relatively dense east-west–trending band of debris-flow source gullies in tributary watersheds of the Santa Ynez Mountains, which appears to correlate with high rainfall amounts of 10.2 mm up to 26.16 mm. In contrast, the 5.1 and 7.6 mm contours define what appears to be the threshold of debris-flow occurrence.

DEBRIS-FLOW DAMAGES

Quantification of debris-flow damages and costs is used for risk assessments, planning for future disasters, and in making decisions about allocating money for pre-disaster mitigation mapping and prevention. However, representing PFDF damages is a challenge because there is no way to quantify the loss of human life, and damages to physical structures are difficult to compile given the variety of entities involved (Taylor and Brabb, 1972; Fleming and Taylor, 1980; and Godt, 1999). Still, damage and cost data are needed to optimize mitigation efforts by comparing the costs of

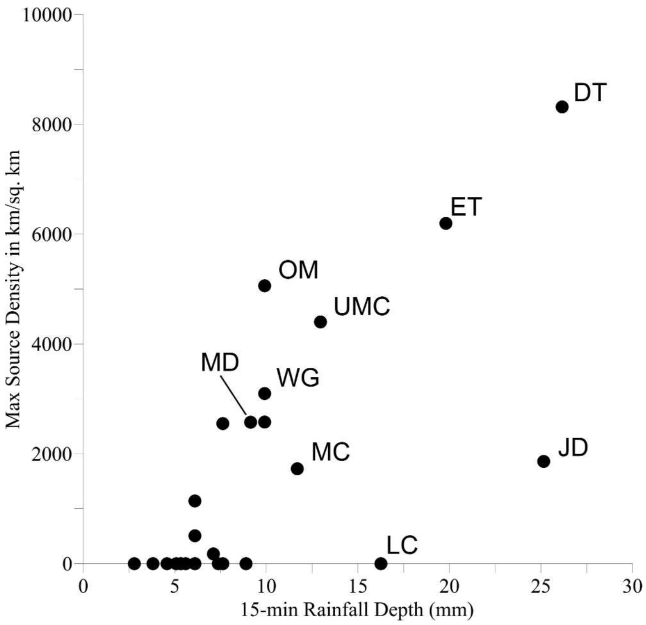

Figure 14. Plot of maximum debris-flow source density against 15 minute rainfall amounts (mm) for the entire burn area using data from Figure 13. Maximum source density was taken as the highest value in length divided by area (km/km^2) within the grid cell in which the rain gauge was located, or within any of the adjacent eight grid cells (Figure 13). The plot shows the dramatic increase in source gully development at depths greater than 5 mm. The rain gauges within the burn perimeter are labeled as follows: DT = Doulton Tunnel, JD = Jameson Dam, ET = Edison Trail, OM = Old Man Mountain, UMC = Upper Matilija Canyon, LC = La Conchita, WG = Wheeler Gorge, MC = Matilija Canyon, MD = Matilija Dam. Low source density corresponding to high rainfall amounts at JD can be explained due to the precipitation gauge being located in the valley away from steeply sloping source areas. Gauge at LC showed features suggesting that debris-flow generation was absent. The cluster of gauges showing 15 minute depths between 2.5 and 10 mm but showing zero debris-flow activity falls within the Sulphur and Santa Paul Ridge areas, south of Ojai and north of Ventura.

damage to the costs of mitigation (McCoy et al., 2016), as well as in addressing risks in economically restricted areas (Santi et al., 2011).

Our compilation of damages and costs followed the general methodology of Fleming and Taylor (1980), including direct, indirect, and undetermined debris-flow damages within Santa Barbara County (damages were unavailable for Ventura County as of January 2020). Direct damages are those necessary to repair and to fully restore all structures and land sustaining physical damage immediately resulting from the debris flows. Indirect damages include secondary losses and results of the debris flows, such as measures taken to mitigate additional damages, and impacts to the local economy from loss of income or taxes. Undetermined damages are those that may be direct or indirect but are inseparable from the Thomas Fire damages based on available information. As there was no significant time separating the events, many losses are reported as a combination of the two events.

Significant structural damage to public and private infrastructure and property occurred within Montecito and in portions of the Carpinteria coastal plain (Figures 6 and 7). Impacts to public infrastructure consisted of seven destroyed and/or damaged bridges along SR 192 and U.S. 101, damages to local water, sewage, gas, and electrical utility infrastructure, and debris deposition in public rights-of-way, debris basins, and channels. Damage to private property was widespread near creek channels, with 558 building structures damaged, more than 162 of which were considered destroyed (CAL FIRE, 2018b). Approximately 2,323 first responders were deployed (SBC, 2018b), which included officers, firefighters, Coast Guard helicopters, armored vehicles, and search and rescue teams with up to 39 search and cadaver dogs, all of whom were involved with 800 rescues, with over 100 rescues done by air (SBC, 2018a, 2018b; Welsh, 2018).

The total estimated direct cost of the debris flows alone, as of January 2020, is $982,950,000, with indirect costs of $49,300,000, and possible additional costs of up to $200,000,000 coming from undetermined costs (Table 6). An additional fluctuating impact is a $330,000,000 reduction in assessed property values as a result of the debris flows (RDN, Inc., 2019). About 67 percent of the direct costs comes from private property insurance claims.

Damages summarized and plotted over a 1/16 km^2 grid (Figure 15) are composed of data from the U.S. Army Corps of Engineers (USACE), Caltrans, Santa Barbara County, the Department of Insurance, and CAL FIRE. USACE debris removal costs directly attributed to 11 debris basins and channels are estimated at over $78,000,000, with additional unattributed county debris removal costs of $24,000,000 (SBCFCD, 2019). A storm clean-up progress map, dated June 2018, was used to delineate the boundaries for debris removal in channels (SBCFCD, 2019). Channels were mapped as polygons approximately bank to bank, for the extents of debris removal, and then intersected by the 1/16 km^2 grid. Bridge repair costs are estimated at $55,000,000 from Caltrans District 5 News Releases (Caltrans, 2018a, 2018b) and are broken down according to local reports (Edhat, 2018). Note, $20 million of this is quoted as a repair contract for five bridges, so this cost was divided equally among these bridges (Caltrans, 2018a; Edhat, 2018).

At the time of this report, the Cal FIRE Damage Inspection Database (DINS) data set provided the most detailed spatial distribution of damaged private structures (CAL FIRE, 2018b). This data set was combined

Table 6. *Summary of direct, indirect, and undetermined costs related to damage caused by 8 January 2018 debris flows in Santa Barbara County.* 7

Damage	Cost (USD 2018)	Data Source
Direct Damage Costs		
U.S. 101 debris removal	$11,250,000	Caltrans (2018a)
Property insurance claims	$658,000,000	Mills et al. (2018)
Debris, basin, and channel removal	$102,000,000	SBCFCD (2019)
County emergency protective measures	$12,600,000	SBCFCD(2019)
Basin and channel permanent restoration	$120,000,000	Horwitz (2018)
SR 192 bridge repairs	$55,000,000	Caltrans (2018b)
County road and bridge repair, 20 miles (32 km)	$8,500,000	SBC Board of Supervisors (2018)
City of Montecito emergency response	$7,000,000	RDN, Inc. (2018)
Water district	$5,500,000	Montecito Water District, (2019)
Sewer district	$1,600,000	Herrick, (2019)
Trail restoration	$1,500,000	Herrick, (2019)
Reduction in assessed property values	$330,000,000	RDN, Inc. (2019)
Indirect Damage Costs		
Lost wages due to U.S. 101 closure	$25,000,000	RDN, Inc. (2018)
New Randall Road debris basin	$20,000,000	Farnsworth (2020)
Installation of 6 debris ring nets	$4,300,000	KSBY (2019)
Undetermined Damage Costs		
SC Edison settlement to public entities	$150,000,000	Yamamura and Smith (2019)
Disaster assistance loans	$50,000,000	U.S. Small Business Administration (2018)
Emergency watershed protection (EWP)	$824,131*	NRCS (2019)

*This value is for the entire fire area.

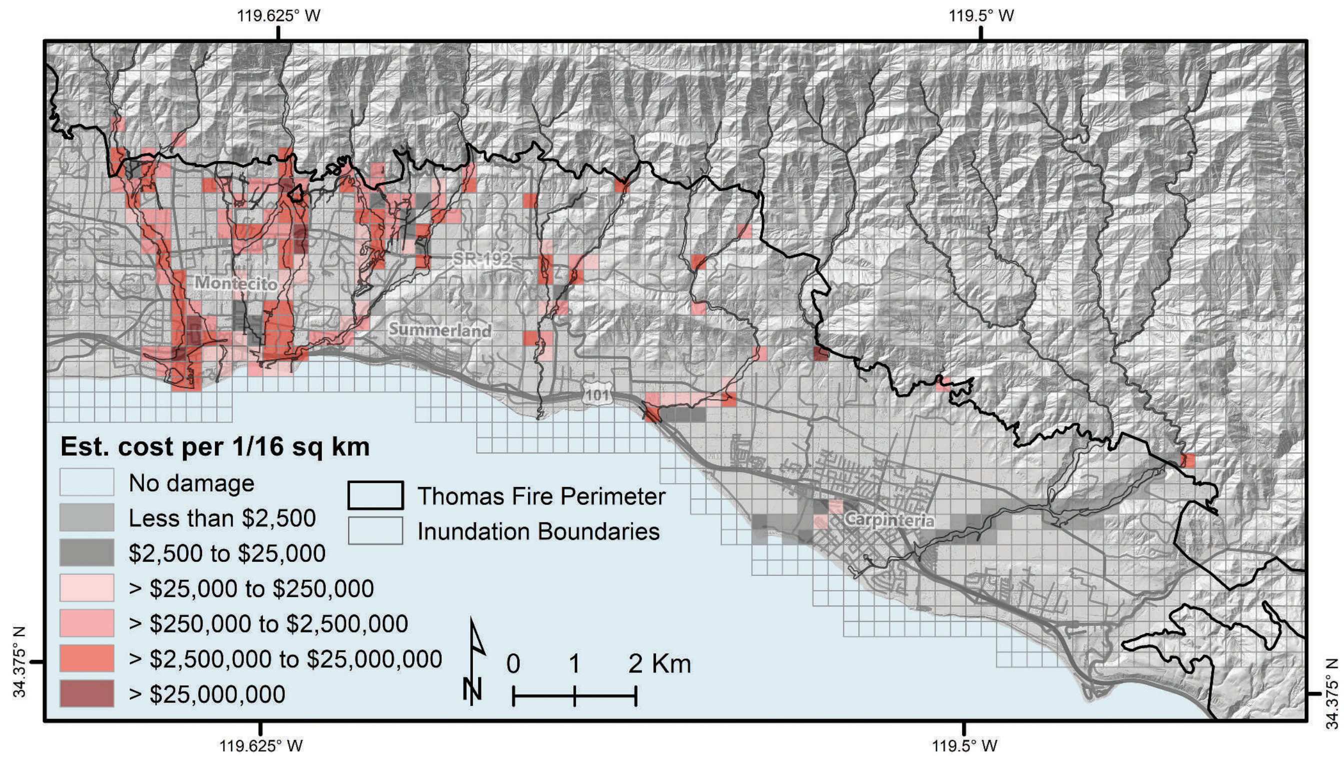

Figure 15. Damage intensity map showing the cumulative estimated cost per 1/16 km^2 grid cell in area impacted by debris-flow deposition. This map includes all direct damages to private property and public infrastructure, including the cost of debris removal. Costs associated with private property are preliminary and based on an evaluation of CAL FIRE DINS data (CAL FIRE, 2018b) as a proxy for final reconstruction costs. The damage data around Carpinteria Salt Marsh Preserve are due to woody debris that issued from Santa Monica and Franklin creeks. Indirect costs, such as economic losses, are not included in this map.

with the $658,000,000 in insurance claims by the Department of Insurance to provide a normalized average cost per damaged structure (Mills et al., 2018), which was calculated as approximately $2,140,482 per destroyed structure, $1,228,795 per highly damaged structure, $436,024 per moderately damaged structure, and $158,554 per slightly damaged structure.

The majority of damage occurred downstream of the burn perimeter in Montecito, Summerland, and Carpentaria, but several structures sustained damage due to debris deposition within the burn perimeter, including buildings on the flanks of Cold Spring Canyon Creek, and the Gobernador Creek Debris Basin. The greatest areas of debris deposition and damage were along Montecito Creek and San Ysidro Creek, with moderate debris deposition and damage along Cold Spring Creek, Hot Springs Creek, Oak Creek, Romero Creek, Toro Canyon Creek, and Arroyo Paredon, the Santa Monica Creek Debris Basin, and the Gobernador Creek Debris Basin. Little deposition occurred in the Franklin Debris Basin and Franklin wash. The geographic intersection of slope with the DINS data (CAL FIRE, 2018b) indicates that 106 of 162 destroyed structures occurred on alluvial fans inclined between 2° and 6° in the general range of surge-front deposition. An additional 26 structures were destroyed on surfaces inclined less than 2°, which shows that surge fronts can be conveyed long distances in confined alluvial channels.

SUMMARY AND CONCLUSIONS

The large-magnitude PFDF of 9 January 2018 claimed 23 lives, damaged or destroyed 558 structures, and caused severe damage to infrastructure in Montecito and Carpinteria, CA. The combination of large, steep watersheds historically susceptible to debris flows positioned above developed alluvial fans of the Santa Barbara Coastal Plain, widespread moderate soil burn severity, and uncommonly intense rainfall immediately following the Thomas Fire was a recipe for disaster. Debris-flow initiation, severity, and distribution were controlled primarily by the track of extreme precipitation associated with the NCFR, causing inundation over a 3.15 km^2 area on the Montecito piedmont and 2.41 km^2 area in Summerland and Carpinteria. Peak-flow depths in these areas were up to 10 m and 5 m, respectively. The total estimated volume of soil, ash, rocks,and woody debris exceeded 1,498,000 m^3 in the Santa Barbara Coastal Plain, which classifies as a magnitude 7 event, if taken as an aggregate (Jakob, 2005), and debris volumes from individual canyons were locally constrained to 21,555 m^3 at west Toro Canyon and 119,271 m^3 at Santa Monica Canyon.

Watershed morphology, geology and soils, and alluvial-fan morphology played important roles in controlling the magnitude, timing, distribution, and runout distance of the debris flows. Watersheds with steep rugged slopes (Melton's number $\geq$0.27) and short planimetric lengths exhibited rapid (5 to 10 minute) response times at Montecito, whereas more gently sloping elongate watersheds (Melton's number $\leq$0.31) with longer lengths ($\geq$6.0 km) at Carpinteria exhibited 30 to 40 minute response times. The dominance of debris-flow behavior, maximum transported boulder size, and runout distance also diminished eastward, mimicking the transition from more debris flow– to streamflow-dominated fans over the same area.

Debris-flow material consisted of a matrix of muddy, ashy sand with gravel derived primarily from rilling of burned hillslopes, and sandstone boulders ranging up to 6 m in diameter derived from alluvial channel deposits. Overbank deposits consisted primarily of boulders and ubiquitous thin patinas of gravelly mud with a durable paste-like consistency.

Destruction was most prominent in Montecito due to avulsions and overbank flows along Montecito, San Ysidro, Oak, Buena Vista, and Romero canyons, which locally followed roads for up to 1 km. Flow severity and damages decreased eastward toward Carpinteria, reflecting the transition of flow behavior below the mountain front from debris flows to sediment-laden flooding, coupled with lower population density and fewer drainage crossings. Where present, existing debris basins reduced surge-front depth maxima and associated impacts on downstream urbanized alluvial fans, but most were not engineered for extreme events.

Preliminary estimates as of January 2020 indicate that this event resulted in direct and indirect costs exceeding $1 billion dollars, but existing data suggest that the final cost may exceed $1.5 billion dollars when all insurance claims are included. Although the January 9 debris-flow event is the most catastrophic on record, multiple watersheds in the same general area were also impacted by debris flows following wildfires in 1964 and 1971, suggesting the average return period for widespread catastrophic debris flows may be less than 20 years.

This event was the result of extreme rainfall on watersheds that were still burning into the winter season, severely stressing the emergency preparedness community and generating a catastrophe on par with the largest magnitude PFDF events documented in California. While in general, the National Weather Service provided adequate forecast lead time, additional recognition of atmospheric conditions that produce extreme high-intensity rainfall is of great importance in a changing climate, as real-time rainfall data cannot provide adequate warning time for debris flows (Kean et al., 2011; Oakley et al., 2017).

ACKNOWLEDGMENTS

We would like to acknowledge the three anonymous peer reviewers for their constructive comments, and those who contributed information and data to this investigation: Jason Kean, Dennis Staley, Jeffrey Coe, and Francis Rengers (collectively co-leading the phase 1 inundation assessment team from the U.S. Geological Survey); Drew Coe and Pete Cafferata (CAL FIRE); Shawn Johnson, Lael Wageneck, and Jon Frye (Santa Barbara County Public Works); Mark Bandurraga, Bruce Rindahl, and Ron Marotto (Ventura County Watershed Protection District); and Larry Gurrola (engineering geologist).

REFERENCES CITED

Alluvial Fan Task Force (AFTF), 2010, *The Integrated Approach: For Sustainable Development on Alluvial Fans*: Water Resources Institute, California State University, San Bernardino, CA, for the California Department of Water Resources, 183 p.

Armanini, A. and Gregoretti, C., 2005, Incipient sediment motion at high slopes in uniform flow condition: *Water Resource Research*, Vol. 41, No. 12, 8 p., https://doi.org/10.1029/2005WR004001.

Bull, W. B., 1977, The alluvial fan environment: *Progress in Physical Geography*, Vol. 1, pp. 222–270.

Burns, M., 2018, *When 'The Big One' Isn't an Earthquake*: Edhat Santa Barbara, January 16, 2018: Electronic document, available at https://www.edhat.com/news/when-the-big-one-isn-t-an-earthquake

Byrne, R., 1979, *Fossil Charcoal from Varved Sediments in the Santa Barbara Channel—An Index of Wildfire Frequencies in the Los Padres National Forest (735–1520 AD)*: Pacific Southwest Forest and Range Experiment Station Report PSW-47, Berkeley, CA, 70 p.

California Department of Forestry and Fire Protection (CAL FIRE), 2018a, *Thomas Fire Watershed Emergency Response Team—Final Report*: California Department of Forestry and Fire Protection, Sacramento, CA, *Report CA-VNC-103156*, 172 p.

California Department of Forestry and Fire Protection (CAL FIRE), 2018b, *Damage Inspection Database (DINS)*: California Department of Forestry and Fire Protection, Office of the State Fire Marshall, Sacramento, CA, ArcGIS files dated 26 April 2018.

California Department of Forestry and Fire Protection (CAL FIRE), 2018c, *Historic Fire Perimeter Database*: Electronic data, available at https://frap.fire.ca.gov/frap-projects/fire-perimeters/

California Department of Water Resources (CADWR), 1973, *California High Water 1971–1972*: California Department of Water Resources, Sacramento, CA, pp. 69–72.

Caltrans, 2018a, News Release, Monday, October 8, 2018: Electronic document, available at http://www.dot.ca.gov/dist05/paffairs/santabarbara/100818.pdf

Caltrans, 2018b, Caltrans Presentation of U.S. 101 recovery to SBCAG Board, February 15, 2018: County of Santa Barbara Access Television, CSBTV20.

Cannon, S. H.; Boldt, E. M.; Kean, J. W.; Laber, J.; and Staley, D.M., 2010, *Relations between Rainfall and Postfire Debris-Flow and Flood Magnitudes for Emergency-Response Planning, San Gabriel Mountains, Southern California*: *U.S. Geological Survey Open-File Report 2010-1039*, 31 p.

Cannon, S. H.; Gartner, J. E.; Parrett, C.; and Parise, M., 2003, Wildfire-related debris-flow generation through episodic progressive sediment-bulking processes, western USA. In Rickenmann, D. and Chen, C. (Editors), *Debris-Flow Hazards Mitigation: Mechanics, Prediction, and Assessment*: Millpress, Rotterdam, Netherlands, pp. 71–82.

Chawner, W. D., 1934, *The Montrose–La Crescenta Flood of January 1, 1934, and its Sedimentary Aspects*: *M.S. Thesis*, California Institute of Technology, Pasadena, CA, 78 p.

Chen, T.; Ren, L.; Yuan, F.; Yang, X.; Jiang, S.; Tang, T.; Liu, Y.; Zhao, C.; and Zhang, L., 2017, Comparison of spatial interpolation schemes for rainfall data and application in hydrological modeling: *Water*, Vol. 9, 18 p., https://doi.org/10.3390/w9050342.

Chow, V. T., 1959, *Open-Channel Hydraulics*: McGraw-Hill Book Company, New York, NY, 680 p.

Coe, J. A.; Godt, J. W.; Parise, M.; and Moscariello, A., 2003, Estimating debris flow probability using fan stratigraphy, historic records, and drainage basin morphology, Interstate 70 highway corridor, central Colorado, U.S.A. In Rickenmann, D. and Chen, C. (Editors), *Debris-Flow Hazards Mitigation: Mechanics, Prediction, and Assessment*: Millpress, Rotterdam, Netherlands, pp. 1085–1096.

Dibblee, T. W., Jr., 1966, *Geology of the Central Santa Ynez Mountains, Santa Barbara County, California*: California Division of Mines and Geology Bulletin 186.

Dibblee, T. W., Jr., 1982, Geology of the Santa Ynez–Topatopa Mountains, southern California. In Fife, D. L. and Minch, J. A. (Editors), *Geology and Mineral Wealth of the California Transverse Ranges*: South Coast Geological Society, Annual Symposium and Guidebook Number 10, Mason Hill Volume, pp. 40–56.

Edhat, 2018, *Caltrans Continues to Rebuild/Repair Bridges on State Route 192*: Edhat Santa Barbara: Electronic document, available at https://www.edhat.com/news/caltrans-continues-to-rebuildrepair-bridges-on-state-route-192

Farnsworth, B., 2020, *Work on Randall Road Debris Basin Expected Summer of 2021*: KEYT News: Electronic document, available at https://keyt.com/news/2020/01/07/randall-road-will-transform-into-a-debris-basin/

Fleming, R. W. and Taylor, F. A., 1980, *Estimating the Costs of Landslide Damage in the United States*: U.S. Geological Survey Circular 832, 21 p.

Gabet, E. J., 2003, Post fire thin debris flows: Sediment transport and numerical modeling: *Earth Surface Processes Landforms*, Vol. 28, pp. 1341–1348.

Gartner, J. E.; Cannon, S. H.; and Santi, P. M., 2014, Empirical models for predicting volumes of sediment deposited by debris flows and sediment-laden floods in the Transverse Ranges of southern California: *Engineering Geology*, Vol. 176, pp. 45–56, https://doi.org/10.1016/j.enggeo.2014.04.008.

Godt, J. W., 1999, *Maps Showing Locations of Damaging Landslides Caused by El Niño Rainstorms, Winter Season 1997–98, San Francisco Bay Region, California*: Pamphlet to accompany U.S. Geological Survey Miscellaneous Field Studies Maps MF-2325-A-J.

Gurrola, L. and Rogers, J. D., 2020, Geologic hazards due to landslide dams in the Cold Springs and Hot Springs watersheds, County of Santa Barbara, California: *Geological Society of America Abstracts with Programs*, Vol. 52, No. 4, paper 26-7.

Herrick, K. M., 2019, Village Beat: The Year in Review 2018: *Montecito Journal*, Vol. 24, No. 52: Electronic document, available at https://issuu.com/santabarbarasentinel/docs/mj_52_24_full

Horwitz, H., 2018, *Santa Barbara County Public Works Responds to Devastating Mudflow*: APWA Reporter, May 2018: Electronic document, available at https://www.apwa.net/Library/Reporter/201805_ReporterOnline.pdf

Hungr, O.; McDougall, S.; Wise, M.; and Cullen, M., 2007, Magnitude–frequency relationships of debris flows and debris avalanches in relation to slope relief: *Geomorphology*, Vol. 96, No. 3–4, pp. 355–365.

Hungr, O.; Morgan, G. C.; and Kellerhals, R., 1984, Quantitative analysis of debris torrent hazards for design of remedial measures: *Canadian Geotechnical Journal*, Vol. 21, pp. 663–677, https://doi.org/10.1139/t84-073.

Iverson, R. M., 1997, The physics of debris flows: *Reviews of Geophysics*, Vol. 35, pp. 245–296.

Iverson, R. M., 2014, Debris flows: Behavior and hazard assessment: *Geology Today*, Vol. 30, No. 1, pp. 15–20, https://doi.org/10.1111/gto.12037.

Jakob, M., 2005, A size classification for debris flows: *Engineering Geology*, Vol. 79, pp. 151–161.

Jakob, M.; Weatherly, H.; Bale, S.; Perkins, A.; and MacDonald, B., 2017, A multi-faceted debris-flood hazard assessment for Cougar Creek, Alberta, Canada: *Hydrology*, Vol. 4, No. 7, 33 p.

Kean, J. W.; McCoy, S. W.; Tucker, G. E.; Staley, D. M.; and Coe, J. A., 2013, Runoff-generated debris flows: Observations and modeling of surge initiation, magnitude, and frequency: *Journal Geophysical Research: Earth Surface*, Vol. 118, pp. 2190–2207, https://doi.org/10.1002/jgrf.20148.

Kean, J. W. and Staley, D. M., 2019, Estimating the annual probability of post-fire debris flow in southern California: *American Geophysical Union, Abstracts with Programs*, abstract
8 NH33E-0968.

Kean, J. W.; Staley, D. M.; and Cannon, S. H., 2011, In situ measurements of post fire debris flows in southern California: Comparisons of the timing and magnitude of 24 debris-flow events with rainfall and soil moisture conditions: *Journal Geophysical Research*, Vol. 116, No. 4, 21 p., https://doi.org/10.1029/2011JF002005.

Kean, J. W.; Staley, D. M.; Lancaster, J. T.; Rengers, F. K.; Swanson, B. J.; Coe, J. A.; Hernandez, J. L.; Sigman, A. J.; Allstadt, K. E.; and Lindsay, D. N., 2019, Inundation, flow dynamics, and damage in the 9 January 2018 Montecito debris-flow event, California, USA: Opportunities and challenges for post wildfire risk assessment: *Geosphere*, Vol. 15, No. 4, pp. 1140–1163, https://doi.org/10.1130/GES02048.1.

Keller, E.; Adamaitis, C.; Alessio, P.; Anderson, S.; Goto, E.; Gray, S.; Gurrola, L.; and Morell, K., 2020a, Applications in geomorphology: *Geomorphology*, Vol. 366, pp. 106729, https://doi.org/10.1016/j.geomorph.2019.04.001.

Keller, E.; Adamaitis, C.; Alessio, P.; Goto, E.; and Gray, S., 2020b, Montecito debris flows of 9 January 2018: Physical processes and social implications. In Heermance, R.V. and Schwartz, J.J. (Editors), *From the Islands to the Mountains: A 2020 View of Geologic Excursions in Southern California*: Geological Society of America Field Guide 59, p. 95–114.

KSBY, 2019, *Montecito Debris Flow Nets Could Be Installed Next Week*: KSBY.com: Electronic document, available at https://ksby.com/news/local-news/2019/04/30/montecito-debris-flow-nets-could-be-installed-next-week

Laber, J., 2018, *An Overview of the January 9, 2018, Flash Flood and Debris Flow Event in Montecito, CA*: Electronic document, available at https://www.alertsystems.org/presentations/Conf2018/Session1-Recent_Events/Laber_REC.pdf

Lamb, M. P.; Dietrich, W. E.; and Venditti, J. G., 2008, Is the critical Shields stress for incipient sediment motion dependent on channel-bed slope?: *Journal Geophysical Research*, Vol. 113, pp. F02008, https://doi.org/10.1029/2007JF000831.

Lancaster, J. T., 2018, *The Santa Barbara County 1/9 Debris Flow of 2018 Extreme Runoff Response to Extreme Precipitation*: Presentation to the Southwest Extreme Precipitation Symposium, La Jolla, CA, March 28, 2018. 9

Lancaster, J. T.; Spittler, T. E.; and Short, W. R., 2015, *Alluvial Fan Flooding Hazards: An Engineering Geology Approach to Preliminary Assessment*: *California Geological Survey Special Report 227*, 46 p.

Lukashov, S. G.; Lancaster, J. T.; Oakley, N. S.; and Swanson, B. J., 2019, Post fire debris flows of 9 January 2018, Thomas Fire, southern California: Initiation areas, precipitation and impacts. In Kean, J. W.; Coe, J. A.; Santi, P. M.; and Guillen, B. K. (Editors) *Debris-Flow Hazards Mitigation: Mechanics, Monitoring, Modeling, and Assessment*: *Proceedings of the Seventh International Conference on Debris-Flow Hazards Mitigation, June 10–13, 2019*: Association of Environmental and Engineering Geologists, Golden, CO, pp. 774–781.

McCoy, K.; Krasko, V.; Santi, P.; Kaffine, D.; and Rebennack, S., 2016, Minimizing economic impacts from post fire debris flows in the western United States: *Natural Hazards*, Vol. 83, pp. 149–176, https://doi.org/10.1007/s11069-016-2306-0.

Mensing, S. A.; Michaelson, J.; and Byrne, R., 1999, A 560-year record of Santa Ana fires reconstructed from charcoal deposited in the Santa Barbara Basin, California: *Quaternary Research*, Vol. 51, pp. 295–305.

Mills, E.; Lamm, T.; Sukhia, S.; Elkind, E.; and Ezroj, A., 2018, *Trial by Fire: Managing Climate Risks Facing Insurers in the Golden State*: California Department of Insurance, Sacramento, CA: Electronic document, available at https://www.law.berkeley.edu/wp-content/uploads/2018/09/Trial-by-Fire-September-2018.pdf

Minor, S. A.; Kellogg, K. S.; Stanley, R. G.; Gurrola, L. D.; Keller, E. A.; and Brandt, T. R., 2009, *Geologic Map of the Santa Barbara Coastal Plain Area, Santa Barbara County, California*: U.S. Geological Survey Scientific Investigations Map 3001, 1 sheet, scale 1:25,000, pamphlet 38 p.

Montecito Water District (MWD), 2019, *Montecito Water District Update*: Montecito Association Board Meeting, February 12, 2019: Electronic document, available at https://www.montecitowater.com/news/presentation-to-montecito-association/

Moody, J. A. and Martin, D. A., 2001, Initial hydrologic and geomorphic response following a wildfire in the Colorado Front Range: *Earth Surfaces Processes Landforms*, Vol. 26, pp. 1049–1070.

National Oceanic and Atmospheric Administration (NOAA), 1971, *Climatological Data*, Vol. 77, No. 12: NOAA, Boulder, CO.

National Research Council (NRC), 1996, *Alluvial Fan Flooding*: Committee on Alluvial Fan Flooding, Water Science and Technology Board, Commission on Geosciences, Environment, and Resources, National Research Council, National Academy Press, Washington, D.C., 172 p.

Natural Resources Conservation Service (NRCS), 2019, personal communication.

Oakley, N. S.; Cannon, F.; Munroe, R.; Lancaster, J. T.; Gomberg, D.; and Ralph, F. M., 2018, Brief Communication: Meteorological and climatological conditions associated with the 9 January 2018 post fire debris flows in Montecito and Carpinteria, California, USA: *Natural Hazards*, Vol. 18, pp. 3037–3043, https://doi.org/10.5194/nhess-18-3037-2018.

Oakley, N. S.; Lancaster, J. T.; Kaplan, M. L.; and Ralph, F. M., 2017, Synoptic conditions associated with cool season post fire debris flows in the Transverse Ranges of southern California: *Natural Hazards*, Vol. 88, pp. 327–354, https://doi.org/10.1007/s11069-017-2867-6.

Perica, S.; Dietz, S.; Heim, S.; Hiner, L.; Maitaria, K.; Martin, D.; Pavlovis, S.; Roy, I.; Trypaluk, C.; Unruh, D.; Yan, F.; Yekta, M.; Zhao, T.; Bonnin, G.; Brewer, D.; Chen, L.; Parzybok, T.; and Yarchoan, J., 2011, *Precipitation-Frequency Atlas of the United States, California*: National Oceanic and Atmospheric Administration Atlas 14, Vol. 6, Version 2.0.

Pierson, T. D. and Costa, J. E., 1987, A rheologic classification of subaerial sediment-water flows. In Costa, J. E. and Wieczorek, G. F. (Editors), *Debris Flows/Avalanches: Process, Recognition, and Mitigation*: Geological Society of America, Reviews Engineering Geology, Vol. 7, pp. 1–12.

Prochaska, A. B.; Santi, P. M.; Higgins, J. D.; and Cannon, S. H., 2008, A study of methods to estimate debris flow velocity: *Landslides*, Vol. 5, pp. 431–444, https://doi.org/10.1007/s10346-008-0137-0.

Robert D. Niehaus, Inc. (RDN, Inc.), 2018, *The Economic Impacts of the Montecito Mudslides: A Preliminary Assessment*: Electronic document, available at http://www.rdniehaus.com/rdn/wp-content/uploads/2018/03/RDN_Montecito_Mudslides_Impacts-1.pdf

Robert D. Niehaus, Inc. (RDN, Inc.), 2019, *The Montecito Debris Flow One Year Later: Housing Market Impact and Recover*: Electronic document, available at http://www.rdniehaus.com/rdn/wp-content/uploads/2019/03/RDN_Montecito-Debris-Flow_Housing-Market-Impact_03-19.pdf

10 Robert D. Niehaus, Inc. (RDN, Inc.), 2020, *Two Years Later: Residential Rebuilding Efforts Since the Montecito Debris Flow*: Electronic document, available at https://www.rdniehaus.com/two-years-later-rebuilding-efforts-since-the-montecito-debris-flow/

Santa Barbara County (SBC), 2018a, *Santa Barbara County 1/9 Debris Flow Disaster Response and Recovery: Central Coast Climate Change Collaborative*, April 24, 2018: Electronic document, available at http://www.centralcoastclimate.org/wp-content/uploads/2018/05/5.-Matt-Pontes.pdf

Santa Barbara County (SBC), 2018b, *Thomas Fire and 1/9 Debris Flow After-Action Report and Improvement Plan*: Electronic document, available at https://www.countyofsb.org/asset.c/4550

Santa Barbara County Flood Control District (SBCFCD), 1969, *1969 Floods*: Electronic document, available at https://www.countyofsb.org/pwd/waterdownloads.sbc

Santa Barbara County Flood Control District (SBCFCD), 2018, personal communication, 130 East Victoria Street Suite 200, Santa Barbara, CA 93101.

Santa Barbara County Flood Control District (SBCFCD), 2019, personal communication, 130 East Victoria Street Suite 200, Santa Barbara, CA 93101.

Santa Barbara County Flood Control District (SBCFCD), 2020, Santa Barbara—Annual Rainfall (Stn #234) 1900–2019: Electronic document, available at https://www.countyofsb.org/pwd/water/downloads/hydro/graphs/234graph.pdf

Santi, P. M.; deWolfe, V. G.; Higgins, J. D.; Cannon, S. H.; and Gartner, J. E., 2008, Sources of debris flow material in burned areas: *Geomorphology*, Vol. 96, pp. 310–321, https://doi.org/10.1016/j.geomorph.2007.02.022.

Santi, P. M.; Hewitt, K.; VanDine, D. F.; and Barillas Cruz, E., 2011, Debris-flow impact, vulnerability and response: *Natural Hazards*, Vol. 56, pp. 371–402.

Scheidl, C. and Rickenmann, D., 2010, Empirical prediction of debris-flow mobility and deposition on fans: *Earth Surface Processes Landforms*, Vol. 35, pp. 157–173.

Schiff, D. and D'Agostino, R. B., 1996, *Practical Engineering Statistics*: John Wiley & Sons, New York, NY, 309 p.

Schwartz, J., 2017, Assessment of the post fire debris flow and flooding events of January 20, 2017 in the Sherpa Fire burned area. In *Diggin' Deep*, No. 313: Minerals & Geology, U.S. Forest Service, Washington, D.C., pp. 9–11. 11

Shuirman, G. and Slosson, J. E., 1992, The fire-flood sequence; a deadly combination. In *Forensic Engineering, Environmental Case Histories for Civil Engineers and Geologists*: Academic Press, San Diego, CA, pp. 186–206.

Staley, D. M.; Kean, J. W.; Cannon, S. H.; Schmidt, K. M.; and Laber, J. L., 2013, Objective definition of rainfall intensity–duration thresholds for the initiation of post fire debris flows in southern California: *Landslides*, Vol. 10, pp. 547–562, https://doi.org/10.1007/s10346-012-0341-9.

Staley, D. M.; Wasklewicz, T. A.; and Kean, J. W., 2014, Characterizing the primary material sources and dominant erosional processes for post-fire debris-flow initiation in a headwater basin using multi-temporal terrestrial laser scanning data: *Geomorphology*, Vol. 214, pp. 324–338.

Taylor, F. A. and Brabb, E. E., 1972, *Maps Showing Distribution and Cost by Counties of Structurally Damaging Landslides in the San Francisco Bay Region, California, Winter of 1968–69*: U.S. Geological Survey Miscellaneous Field Studies Map MF-327.

U.S. Army Corps of Engineers Los Angeles District (USACE), 1974, *Flood Plain Information, Montecito Streams, Vicinity of Montecito, Santa Barbara, County, California*: USACE, Department of the Army, Washington, D.C., 37 p.

U.S. Army Corps of Engineers Los Angeles District (USACE), 1999, *Santa Barbara County Streams, Lower Mission Creek Flood Control Feasibility Study, Draft Main Report & EIS/EIR*: USACE, Department of the Army, Washington, D.C., 39 p.

U.S. Army Corps of Engineers Los Angeles District (USACE), 2018, *Debris Basins, Santa Barbara County, CA January 16, 2018*: Electronic document, available at https://www.spl.usace.army.mil/Missions/Emergency-Management/Santa-Barbara-County-Debris-Removal/

U.S. Geological Survey (USGS), 2005, *Southern California—Wildfires and Debris Flows*: U.S. Geological Survey Fact Sheet 2005-3106.

U.S. Geological Survey, 2019, *Quaternary Fault and Fold Database for the United States*: Electronic data, available at https://earthquake.usgs.gov/hazards/qfaults/

U.S. Small Business Administration (SBA), 2018, *SBA Tops $50 Million in Disaster Assistance Loans*: Disaster Press Release CA 15438-05: Electronic document, available at https://www.sba.gov/offices/disaster/dfocw/resources/1624696

Wagner, D. L.; Lancaster, J. T.; and DeRose, M., 2012, *The Oak Creek Debris and Hyperconcentrated Flows of July 12, 2008, Inyo County, California: A Geologic Investigation: California Geological Survey Special Report 225*, 63 p.

Wells, W. G., 1987, The effects of fire on the generation of debris flows in southern California: *Reviews in Engineering Geology*, Vol. 7, pp. 105–114., https://doi.org/10.1130/REG7-p105.

Welsh, A. and Davies, T., 2011, Identification of alluvial fans susceptible to debris-flow hazards: *Landslides*, Vol. 8, pp. 183–194, https://doi.org/10.1007/s10346-010-0238-4.

Welsh, N., 2018, Search dogs comb hills of Montecito for survivors and remains: *Santa Barbara Independent*, 14 January 2018: Electronic document, available at https://www.independent.com/2018/01/14/search-dogs-comb-hills-montecito-survivors-and-remains/

Western Regional Climate Center (WRCC), 2017, *Cooperative Climatological Data Summaries*: Electronic data, available at https://wrcc.dri.edu/cgi-bin/cliMAIN.pl?ca0619

Wilford, D. J.; Sakal, M. E.; Innes, J. L.; Sidle, R. C.; and Bergerud, W. A, 2004, Recognition of debris flow, debris-flood and flood hazard through watershed morphometrics: *Landslides*, Vol. 1, pp. 61–66.

Williams, A. P.; Abatzoglou, J. T.; Gershunov, A.; Guzman-Morales, J.; Bishop, D. A.; Balch, J. K.; and Lettenmaier, D. P., 2019, Observed impacts of anthropogenic climate change on wildfire in California: *Earth's Future*, Vol. 7, pp. 892–910, https://doi.org/10.1029/2019EF001210.

Wills, C. J.; Roth, N. E.; McCrink, T. P.; and Short, W. R., 2017, The California landslide inventory database. In DeGraff, J. and Shakoor, A. (Editors), *Proceedings of the Third North American Symposium on Landslides*: Association of Environmental and Engineering Geologists, Roanoke, VA, pp. 666–674.

Yamamura, J. and Smith, D., 2019, Santa Barbara City and County part of $360 million Edison settlement: *Santa Barbara Independent*, 13 November 2019: Electronic document, available at https://www.independent.com/2019/11/13/santa-barbara-city-and-county-part-of-360-million-edison-settlement/

Authors Queries

Journal: **Environmental and Engineering Geoscience**
Paper: **EEGS-26-04-04_1XO**
Title: **Observations and Analyses of the 9 January 2018 Debris-Flow Disaster, Santa Barbara County, California**

Dear Author
During the preparation of your manuscript for publication, the questions listed below have arisen. Please attend to these matters and return this form with your proof. Many thanks for your assistance

Query Reference	Query
1	AU: Please provide email address for corresponding author in footnote. Copy editor
2	AU: You cite Staley (2018) in the first paragraph of the text. This is not listed in the reference list. Please provide full matching reference for the list or revise in-text citation to match a reference already in the list. Copy editor
3	AU: CGS (2005) is cited in the caption for Figure 6: This is not listed in the reference list. Please provide full matching reference for the list or delete citation in the caption. Copy editor
4	AU: You cite CAL FIRE (2018) in the caption for Figure 11: Please specify 2018a, 2018b, 2018c, or a combination. Copy editor
5	AU: You cite CAL FIRE (2018) in the caption for Table 5: Please specify 2018a, 2018b, 2018c, or a combination. Copy editor
6	AU: You cite CAL FIRE (2018) in the caption for Figure 13: Please specify 2018a, 2018b, 2018c, or a combination. Copy editor
7	AU: You cite SBC Board of Supervisors (2018) in Table 6: This is not listed in the reference list. Please provide matching reference for the list or delete citation in the table. Copy editor
8	AU: Please list volume number for Kean and Staley (2019) reference. Copy editor
9	AU: Please list editors, title, and type of volume (proceedings?), publisher, and place of publication for Lancaster (2018) reference. Copy editor
10	AU: RND, Inc. (2020) is listed in the reference list but is not cited in the text, figure captions, or tables. Please add in-text citation or delete reference from the list. Copy editor
11	AU: Please list editors (if any) for volume in Schwartz (2017) reference. Copy editor